

Abstract

Title: An Analysis of Thermally Induced Arcing Failure of Electrical Cable

Ryan Patrick Fisher, Master of Science, 2013
University of Maryland

Directed By: Dr. Stanislav I. Stoliarov
Department of Fire Protection Engineering

Arc failure of Southwire Romex Simpull non-metallic sheathed 14/2 American wire gauge (AWG) with ground cable due to external heat was examined. This type of cable was selected due to its widespread use in residential building wiring. This research is motivated by the fact that currently there are no widely accepted methods or models used to predict electric arc failure in cables exposed to thermal conditions or to determine whether an arc failure event was the cause or result of a fire. A variety of tests were performed at various temperatures to learn more about the arc failure of these cables. The cables were exposed to precise temperatures with a steady heating rate in a convection oven in order to best attempt to eliminate heat transfer through the cable. In order to explore the effect current may have on the time to arc failure of the cable, experiments at different temperatures were performed in both loaded and unloaded scenarios. During many of these tests, voltage and current measurements were collected during an arcing event. As part of the process of exploring the events leading up to arc failure, electrical resistance tests of the cable's insulation components were examined. A model was developed to predict time to arc failure at a variety of temperatures based on thermal degradation of the PVC insulation. The purpose of the developed model is to be able to predict cable failure based on known thermal conditions. The proposed values of the model developed are in examining a prior thermally induced electrical arcing incident or in determining the suitability of a cable in an abnormal thermal environment. The results of this research will be useful in continuing the research and education of the arc failure of electrical cables.

AN ANALYSIS OF THERMALLY INDUCED ARCING FAILURE OF ELECTRICAL CABLES

By
Ryan Fisher

Thesis submitted to the Faculty of the Graduate School of the
University of Maryland, College Park in partial fulfillment
of the requirements for the degree of
Master of Science
2013

Committee:

Professor Stanislav Stoliarov, Chair
Professor James Milke
Professor James Quintiere

© Copyright
by
Ryan Fisher
2013

ACKNOWLEDGEMENTS

I would like to thank all of the people who assisted me during the process of this research study. First and foremost, I would like to thank Dr. Stoliarov for the incredible amount of assistance he gave to me throughout this project. His patience, understanding, and wisdom helped to keep this project heading in the right direction. I have been fortunate to learn under Dr. Stoliarov on several projects at the University of Maryland, all of which were successful due in large part to his efforts. Mike Keller and his associates at the Bureau of Alcohol, Tobacco, and Firearms and Explosives were extraordinarily helpful in providing their expertise, insight, and equipment to this project. Their knowledge was essential in the success of this project.

I would also like to thank Olga Zeller for the continuous support she gave throughout the fire protection engineering lab. Without her help, my progress in the lab would have been slowed greatly for Olga was always there to assist me with any problem I was experiencing.

Finally, I would like to thank my fellow classmates in the Fire Protection Engineering Department who supported me and this project in various ways throughout the entire process.

TABLE OF CONTENTS

Acknowledgements.....	i
List of Tables.....	ii
List of Figures.....	iii
1. Introduction	
1.1 Relevance of Research.....	1
1.2 Electrical Arcing.....	1
1.3 Background Information.....	3
1.4 Purpose of Study.....	4
2. Materials and Methods	
2.1 Materials	
2.1.1 Cable Description.....	5
2.1.2 Oven Description/Temperature Programs.....	6
2.1.3 Power Analyzer.....	9
2.2 Cable Tests	
2.2.1 Cable Testing Setup.....	9
2.2.2 Cable Resistance Tests.....	11
2.2.3 Energized, Unloaded Tests.....	11
2.2.4 Sharp Bends Tests.....	12
2.2.5 Energized, Loaded Tests.....	13
2.2.6 Added Insulation Tests.....	14
2.2.7 Temperature Analysis of Cables	14
2.3 Insulation Component Tests	
2.3.1 Resistance Drop Testing.....	15
2.3.2 Energized Tests.....	17
2.3.3 Ground Paper Sheathing Removed Tests.....	17

2.4 Insulation Component Mass Loss Analysis (TGA).....	18
2.5 Modeling Approach.....	18
3. Results	
3.1 Cable Tests	
3.1.1 Cable Resistance Tests.....	20
3.1.2 Cable Deterioration Observations.....	21
3.1.3 Energized, Unloaded Tests.....	22
3.1.4 Arcing Observations.....	25
3.1.5 Added Insulation Tests.....	26
3.1.6 Sharp Bends Tests.....	27
3.1.7 Energized, Loaded Tests.....	28
3.1.8 Temperature Analysis of Cables.....	30
3.2 Insulation Component Tests	
3.2.1 Resistance Drop Test.....	35
3.2.2 Energized Tests.....	37
3.2.3 Ground Paper Sheathing Removed Tests.....	38
3.4 Insulation Component Mass Loss Analysis (TGA).....	39
4. Modeling Results.....	44
5. Conclusions.....	56
6. Future Work.....	58

Appendix

Model Input Files

Model Time to Arc Failure Predictions

Additional Photographs

References

LIST OF TABLES

<i>Table 1: 230°C Average Time to Resistance Drop.....</i>	<i>20</i>
<i>Table 2: Energized, Unloaded Time to Arc Failure.....</i>	<i>23</i>
<i>Table 3: Cable Geometry Time to Failure Comparison.....</i>	<i>27</i>
<i>Table 4: 200°C Unloaded and Loaded Time to Failure Comparisons.....</i>	<i>28</i>
<i>Table 5: 200°C Cable Internal Temperatures.....</i>	<i>30</i>
<i>Table 6: 230°C Component Time to Resistance Drop Tests.....</i>	<i>36</i>
<i>Table 7: 230°C Component Time to Resistance Drop Tests w/ Combination.....</i>	<i>36</i>
<i>Table 8: 230°C Component Time to Resistance Drop, Arc Failure Comparisons.....</i>	<i>38</i>
<i>Table 9: Removed Ground Paper Sheathing Time to Arc Failure.....</i>	<i>39</i>
<i>Table 10: Insulation Component Arrhenius parameters.....</i>	<i>44</i>
<i>Table 11: Component Degrees of Degradation at Arc Failure.....</i>	<i>50</i>
<i>Table 12: Energized, Loaded Cable Temperature Corrections.....</i>	<i>55</i>
<i>Table 13: Model Time to Failure Predictions (Appendix)</i>	
<i>Experimental Data and Results Tables (Appendix)</i>	

LIST OF FIGURES

<i>Figure 1: Southwire Romex Simpull Non-metallic Sheathed 14/2 with Ground Cable.....</i>	<i>5</i>
<i>Figure 2: Internal Cable Structure.....</i>	<i>6</i>
<i>Figure 3: Oven Temperature Programs.....</i>	<i>8</i>
<i>Figure 4: Cable Testing Schematic.....</i>	<i>10</i>
<i>Figure 5: Cable Mold.....</i>	<i>11</i>
<i>Figure 6: Sharp Bend Testing</i>	<i>13</i>
<i>Figure 7: Insulation Component Test Set Up.....</i>	<i>16</i>
<i>Figure 8: Cable Insulation Components.....</i>	<i>16</i>
<i>Figure 9: 230°C Inverse Normalized Resistance.....</i>	<i>21</i>
<i>Figure 10: General Progression of the Cable Degradation Process.....</i>	<i>22</i>
<i>Figure 11: Cable Arc Aftermath.....</i>	<i>23</i>
<i>Figure 12: Energized, Unloaded Cable Time to Arc Failure.....</i>	<i>24</i>
<i>Figure 13: Energized, Unloaded Cable Arc Current Signature.....</i>	<i>25</i>
<i>Figure 14: Arcing Event.....</i>	<i>26</i>
<i>Figure 15: Energized, Loaded Cable Arc Current Signature.....</i>	<i>29</i>
<i>Figure 16: 200°C Time to Arc Failure Times per Load.....</i>	<i>29</i>
<i>Figure 17: 200°C Energized, Unloaded Cable Temperature Rise.....</i>	<i>32</i>
<i>Figure 18: 210°C Energized, Unloaded Cable Temperature Rise.....</i>	<i>33</i>
<i>Figure 19: 230°C Energized, Unloaded Cable Temperature Rise.....</i>	<i>33</i>
<i>Figure 20: 200°C Energized, 12 Amp Loaded Cable Temperature Rise.....</i>	<i>34</i>
<i>Figure 21: 200°C Energized, 18 Amp Loaded Cable Temperature Rise.....</i>	<i>34</i>
<i>Figure 22: 230°C Insulation Component Inverse, Normalized Resistance.....</i>	<i>35</i>
<i>Figure 23: PVC-Paper Component Post Resistance Testing</i>	<i>37</i>
<i>Figure 24: Outer PVC Mass – TGA.....</i>	<i>40</i>
<i>Figure 25: Outer PVC Mass Loss Rate – TGA.....</i>	<i>40</i>
<i>Figure 26: Inner PVC Mass – TGA.....</i>	<i>41</i>

<i>Figure 27: Inner PVC Mass Loss Rate – TGA.....</i>	<i>41</i>
<i>Figure 28: Paper Mass – TGA.....</i>	<i>42</i>
<i>Figure 29: Paper Mass Loss Rate – TGA.....</i>	<i>42</i>
<i>Figure 30: Nylon Mass – TGA.....</i>	<i>43</i>
<i>Figure 31: Nylon Mass Loss Rate – TGA.....</i>	<i>43</i>
<i>Figure 32: Outer PVC Model Mass Fit.....</i>	<i>45</i>
<i>Figure 33: Outer PVC Model Mass Loss Rate Fit.....</i>	<i>45</i>
<i>Figure 34: Inner PVC Model Mass Fit.....</i>	<i>46</i>
<i>Figure 35: Inner PVC Model Mass Loss Rate Fit.....</i>	<i>46</i>
<i>Figure 36: Nylon Model Mass Fit.....</i>	<i>47</i>
<i>Figure 37: Nylon Model Mass Loss Rate Fit.....</i>	<i>47</i>
<i>Figure 38: Paper Model Mass Fit.....</i>	<i>48</i>
<i>Figure 39: Paper Model Mass Loss Rate Fit.....</i>	<i>48</i>
<i>Figure 40: Model, Experimental Time to Failure Predictions (1).....</i>	<i>53</i>
<i>Figure 41: Model, Experimental Time to Failure Predictions (2).....</i>	<i>53</i>
<i>Figure 42: Model, Loaded Experimental Time to Failure Predictions.....</i>	<i>55</i>
<i>Figure 43: Correct Model, Loaded Experimental Time to Failure Predictions.....</i>	<i>56</i>
<i>Figure 44: Bubbled, Cracked Outer Insulation (Post Exposure) (Appendix)</i>	
<i>Figure 45: Interior Cable Structure (Appendix)</i>	
<i>Figure 46: Component Testing Setup (Appendix)</i>	
<i>Figure 47: Post Arc Failure (Destroyed hot and ground wires) (Appendix)</i>	
<i>Figure 48: PVC-Paper Combination Testing (Post Exposure) (Appendix)</i>	
<i>Figure 49: Copper Beads Ejected From Cable During Arc Failure (Appendix)</i>	

INTRODUCTION

Relevance of Research

Electrical wiring is cited as the cause of many residential fires in the United States. From 2006 to 2008, about 6% of residential fires were categorized as electrical fires. Of those electrical fires, an estimated 40% were attributed to wiring of the building. The rest of the electrical residential fires were attributed to cords, plugs, sockets/receptacles, lighting, and other electrical sources [1]. Per fire, electrical fires were more deadly, caused more injuries, and resulted in more property damage than other nonelectrical fires from 2003 to 2005 [2]. As the statistics show, electrical fires, specifically those caused by building wiring, are still a significant problem in residential fires.

Understanding whether an electric arc is the source of ignition in a residential fire or simply a result of an already existent fire has been a problem for many in the fire investigation community [3]. An electrical arc is described as an electric discharge across a gap or through a semi-conductive medium [4, 5]. Many researchers have made attempts to distinguish between the arc beads of these different types of arcing events, but many attempts have been unsuccessful or unable to be repeated by other researchers. Arc beads produced in these two different scenarios are sometimes referred to as “cause” beads (scenario in which an arc is the cause of a fire) and “victim” beads (where the arc is a result of a nearby fire). The ability to make a distinction between these two types of arc beads is a rather controversial topic [3].

Electrical Arcing

For residential purposes, arc faults can be broken down into two main categories: series or parallel arcing faults. A series arc fault “is an unintended arc in series with either the line wire

or the neutral wire with respect to the load current” [10]. Series arc faults can be produced by loose connections which produce glowing contacts and continuous arcing through char [10].

The types of arc faults of concern for this study are parallel arc faults. Parallel arc faults are caused by an arc between the hot/line or neutral wire and the ground wire [10]. The parallel arc occurs when a “bridge” between the line, ground, or neutral wire exists. This can be caused by direct physical contact between the wires or by a different indirect means. For instance, when the wire insulation in the cable is degraded thermally, there exists a state at which electricity can flow through the compromised insulator. As a result, a parallel arc occurs between the two wires through the compromised insulation. The arc between the two wires produces a large current fault and visually, large sparks are observed. These sparks are small pieces of molten copper that are ejected from the copper wires in the cable due to the high energy event.

If researchers and professionals in the fire investigation community were able to better understand how the electrical arcing event occurs when a cable is exposed to heat, they may be better able to determine if an arc was in fact the source of ignition or a result of an already existent fire. Additionally, if the time to arc failure of electrical wiring when exposed to thermal conditions could be successfully predicted and modeled, it would serve as a powerful tool in the process of determining cause in a fire investigation. In a post-fire scenario, a model capable of using prescribed heating conditions in a space may be able to rule out an electric arc event as a result of thermal conditions being the cause of a fire. Additionally, a model capable of using thermal conditions to predict arc failure based on the material composition of the cable insulation components would be useful in designing cables for use in specific, abnormal thermal applications.

Background Information

A study was performed by the Nuclear Regulatory Commission (NRC) in conjunction with the National Institute of Standards and Technology (NIST) and Sandia National Laboratories to explore thermally induced electrical failure of cables [6,7,8]. A model was developed by the group to predict thermally induced electrical failure. One of the key assumptions of their model is that “electrical failure occurs when the temperature just inside the cable jacket reaches an experimentally determined value” [8]. The data in which the NRC and NIST model is based on is from testing that was performed at Sandia National Laboratories. The cables were heated at a rate specifically to cause electric arcing failure within 10-30 minutes [6,7,8]. As opposed to the NRC/NIST study, a slower and more uniform heating approach was used in this study

An additional modeling study was performed by Anna Matala and Simo Hostikka and presented at the 20th International Conference on Structural Mechanics in Reactor Technology titled *Probabilistic Simulation of Cable Fires in a Cable Tunnel* [9]. In the study, the definition of cable failure was described as when the cable insulation layer reached a temperature of either 180°C or 220°C (both temperature thresholds were considered) [9]. It is not known how the researchers decided to consider those two temperatures for describing electrical arcing failure. Their research was designed to estimate cable failure probabilities in the case of a cable fire starting from a sub-system power cable [9]. The cables described in their modeling approaches consisted of mostly the same insulation and conductor components as those in this study.

The previous two studies discussed made the assertion that electrical cable failure can be described using a threshold cable failure temperature. Part of this study is to determine whether

or not the time of thermal exposure may also play a role in the process leading up to an electrical arc failure.

Purpose of Study

The purpose of this study was to further explore and examine the arc failure of common residential building wiring when exposed to thermal conditions. This research was performed in order to gain a better understanding of when cables fail due to arcing under thermal conditions, what role loaded cables may have on failure as opposed to unloaded cables, and the key components of an arcing event. A loaded cable refers to a cable with current flow (electrical load), and an unloaded cable refers to a cable without any current flowing; unloaded cables are still energized for these experiments. An energized cable refers to one in which voltage is applied.

Information and data from this study will allow for more extensive research on the subject to be performed, will benefit in understanding electrical arc failure under thermal conditions, and will have use in the field of fire investigation. The goals of this research are to gain a better understanding of electric arc failure in cables under thermal conditions and to develop a method or model for predicting the electric arc failure of 14/2 AWG with ground Southwire Romex Simpull non-metallic sheathed cable under thermal conditions.

2 MATERIALS AND METHODS

2.1 Materials

2.1.1 Cable Description

The cable type selected in this study is commonly used in residential branch circuit wiring and is readily available. The specific type of cable used was 14/2 AWG (1.63 mm diameter copper wire) with ground Southwire Romex Simpull non-metallic sheathed cable. A 250' roll of this cable is shown in Figure 1.



Figure 1: Southwire Romex Simpull non-metallic sheathed 14/2 with ground cable

Figure 2 shows the structure of the cable used. The cable consists of three copper wiring elements. The line/hot and neutral wires are sheathed in either black or white polyvinylchloride (PVC), respectively, which is in turn sheathed by clear polyamide (nylon). The ground/grounding wire is wrapped in paper sheathing. In addition to the individual wire

insulations, the three wires are collectively wrapped in a paper layer and then an additional white outer PVC insulation [11].

After purchasing new rolls of cable, the cable was inspected for any obvious deficiencies or deviations from previous rolls of cable. No deficiencies or major deviations were discovered. Throughout the testing, three different packages of 250' rolls of cable were used. All rolls were the same type of cable from the same manufacturer. There may be minor variances in the precise make-up of the cables, but nothing major was observed during inspection.

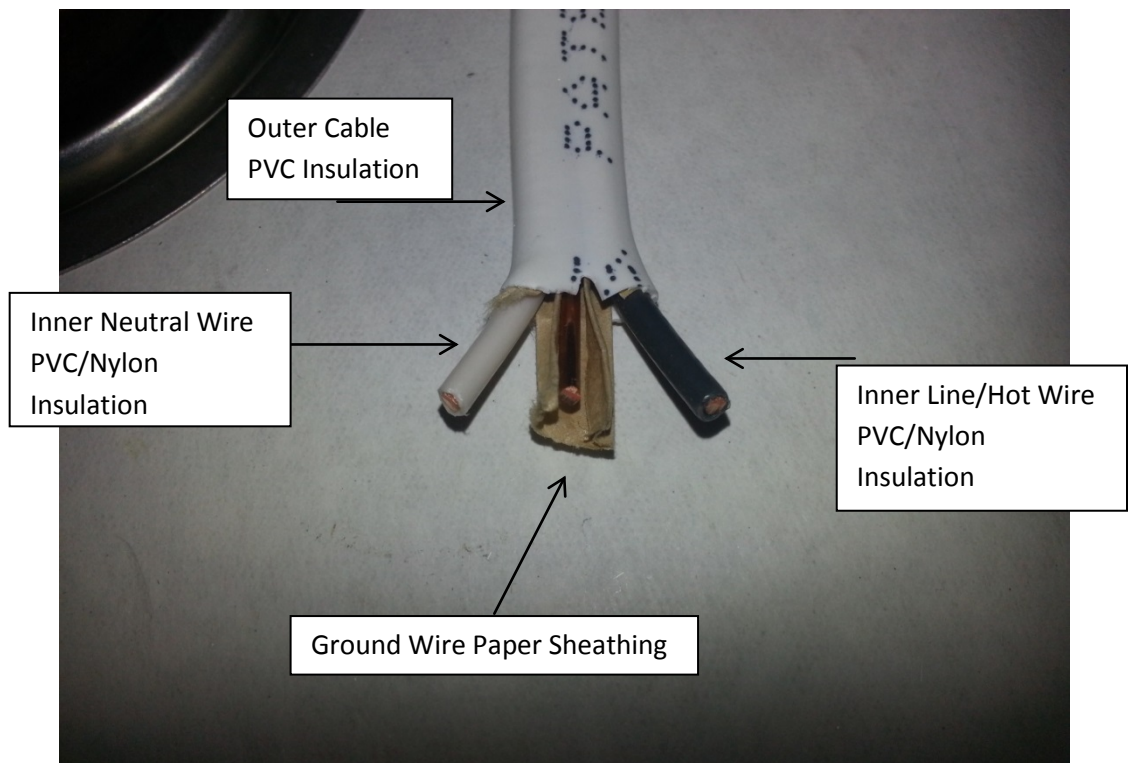


Figure 2: Internal Cable Structure

2.1.2 Oven Description/Temperature Programs

The oven used for the experiments in this study was a convection oven with precise temperature controlling. Three main temperature programs were utilized in the experiments. The

main temperatures used were 200°C, 210°C, and 230°C. These temperatures were chosen due to the fact that full tests could be run within one day. The temperature ramps used were that of the maximum capacity of the oven at each given temperature. In other words, this was the fastest the oven could reach each given temperature. Overall, however, the ramps are relatively slow which allows for even heating throughout the cable. The corresponding oven temperature programs can be seen in Figure 3.

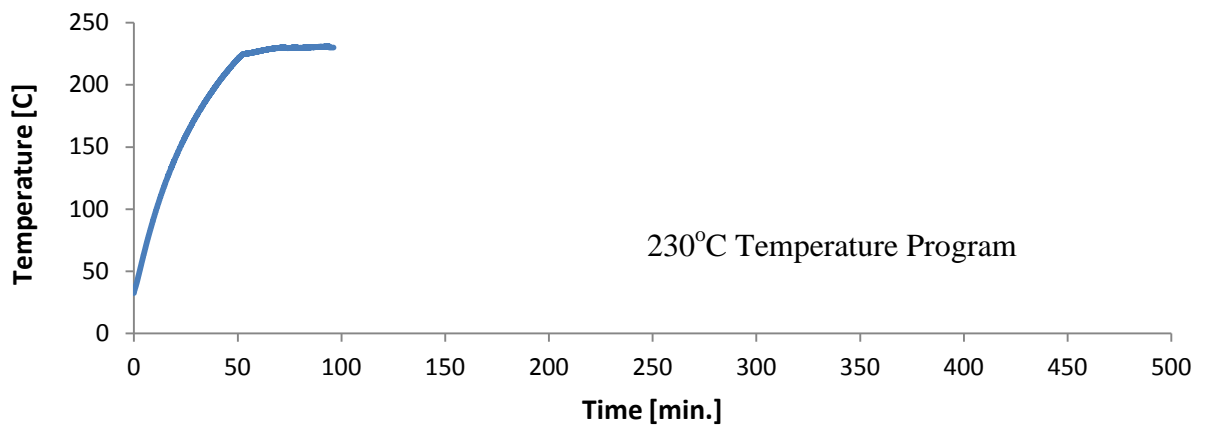
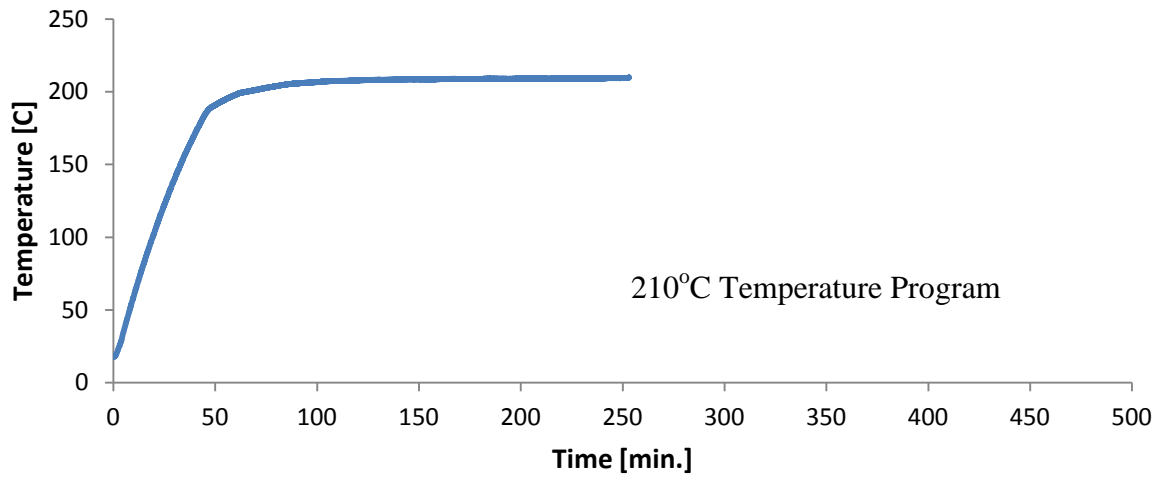
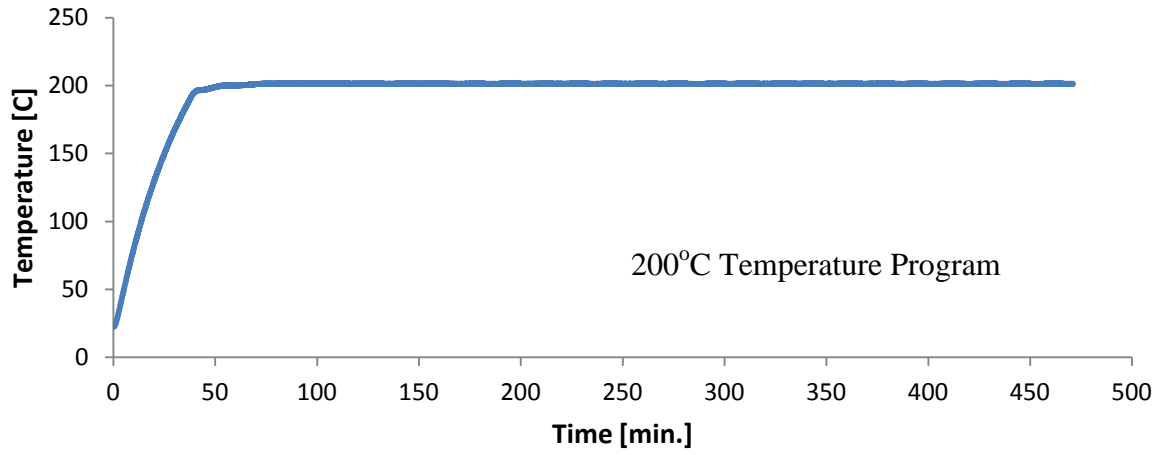


Figure 3: Oven Temperature Programs

2.1.3 Power Analyzer

During these experiments, a Synergy P Portable Data Acquisition System manufactured by Hi-Techniques, Incorporated was connected to the circuit to monitor the current before and during the electrical arcing events. The power analyzer was set to record at a rate of 1000 Hz.

2.2 Cable Tests

2.2.1 Cable Testing Setup

In order to simulate the aging or deterioration of the cable insulation, cable is placed into an oven capable of applying a range of temperatures up to 250° C. The high temperature the cable is exposed to causes the insulation components to degrade, and at a certain instance in time, an electric arc to occur. The cable begins at the wall outlet that provides 120 VAC and continues into the oven where it is exposed to elevated temperatures. Between the wall and the oven there is a 15 Amp General Electric single pole circuit breaker and a 20 Amp fuse in place to provide additional elements of safety when the arc forms. In every region where the cable comes in contact with the oven, the cable is wrapped in a high temperature electrical insulation in order to prevent any wiring from contacting the oven. Figure 4 is a schematic of the experimental set up. 50 inches of cable was placed into the oven in a mold like is seen in Figure 5. The mold is made of thick Kaowool insulation board and the cable is placed flat against the Kaowool board. The cable is secured with metal brackets with a piece of glass wool placed between the metal brackets and the cable. The cable arrangement shown in Figures 4 and 5 is used for all full-length cable experiments. This arrangement allows for a uniform and repeatable test set up. Each different testing method performed in this study (unless otherwise noted), consisted of seven experiments.

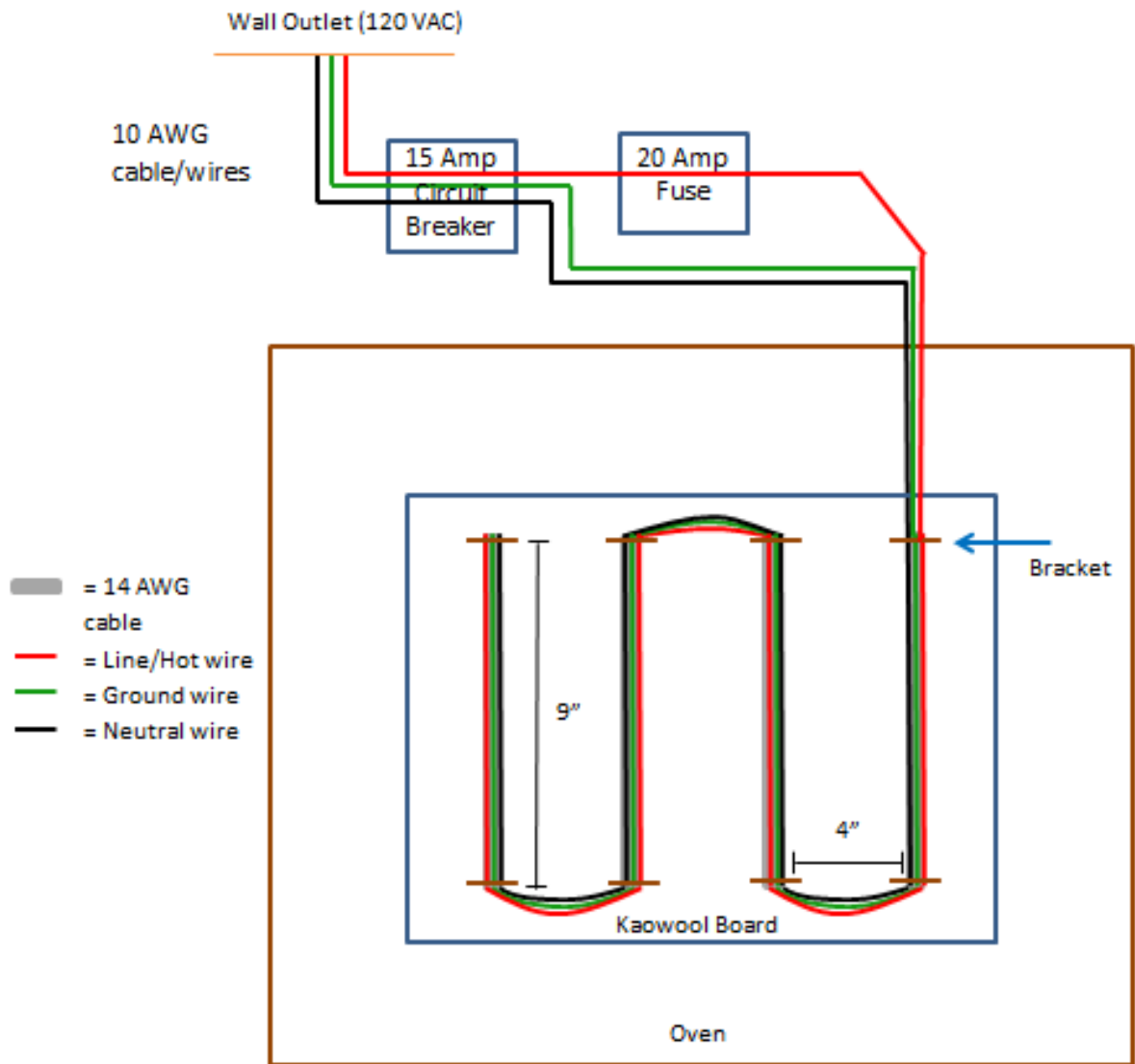


Figure 4: Cable Testing Schematic



Figure 5: Cable Mold

2.2.2 Cable Resistance Tests

The first step of testing involved monitoring the time in which a measurable resistance between the line/hot wire and the ground wire could be determined. This was performed at the 230°C temperature profile with the generic cable set up of Figure 4; the time at which a measurable resistance between two of the wires was recorded.

2.2.3 Energized, Unloaded Tests

The next step in the experimentation was to connect the cable to an energized source. While the cable is energized, there is no current flow for this set of experiments. The purpose of these experiments is to determine the variability in the time to an arcing event at a given temperature. The time to resistance drop with the 230°C profile will be compared with the time to arc failure at the same 230°C temperature profile. Full data sets of seven tests for energized,

unloaded experiments were performed at 200°C, 210°C, and 230°C. During these experiments the power analyzer was used to take current measurements.

2.2.4 Sharp Bends Tests

In order to examine the possible effects of the geometry of the cable set up, a different cable arrangement was explored. In this set of experiments, sharp bends were introduced in the geometry of the cable set up as seen in Figure 6. The cable length was 50” just as it was in previous cable tests, but now bent sharply. This allowed the researchers to examine how an increase in mechanical stress on the cable may have an impact on the time to arc failure. It was hypothesized that sharp bends in the cable could cause the cable to be more susceptible to an electrical arc across the insulation components due to the mechanical stress on the insulation coupled with the thermal degradation of the insulation. Specifically, damaging the structure of the ground paper sheathing was hypothesized to play a role in the time to arc failure. The sharp bends were explored in order to see if a difference in orientation and contact between the PVC insulation and the paper would have an effect on the time to arc failure of the cable.



Figure 6: Sharp Bend Testing. Note: Brown paper pieces used for insulation from fasteners

2.2.5 Energized, Loaded Tests

Energized, loaded cables were also examined. The same set up was used for this set of testing as for the generic cable test set up (excludes the sharp ends testing). However, this set introduced a current flow to the circuit. These tests were used to compare results with the energized, unloaded cable tests as well as work to provide a scenario that will also be encountered in a residence. To determine whether the presence of current flow impacts the time to arc failure for this given set up, a series of seven tests were performed at 200°C. As was performed in the energized, unloaded testing, the power analyzer was connected to the circuit to monitor current throughout the test

2.2.6 Added Insulation Tests

In residential construction, the branch circuit wiring is often surrounded by fiberglass insulation. To explore the impact of such a scenario on an energized, loaded cable thick fiberglass insulation was laid on top of the cable. The geometry of the cable set up was the standard geometry as is depicted in Figures 4 and 5. The hypothesis being tested here is whether or not the insulation plays a significant role in preventing the heat/energy from the current flow within the cable from dissipating. The cable was loaded to 100% of its rated continuous load of 12 Amps.

2.2.7 Temperature Analysis of Cables

During the full cable experiments in the oven, temperature measurements were taken in the cable. Measurements were made using Type K Thermocouples. A thermocouple was placed just beneath the outer PVC insulation, but did not penetrate the paper sheathing that is inside of the outer PVC insulation that surrounds the cable. Care was taken to not puncture any of the inner insulation components with the thermocouple. In the 230°C experiments, this measurement location was on the top surface of the cable. In the 200°C and 210°C experiments, the location for temperature measurement was changed to the underside of the cable between the cable and the insulation board. The same method of placing a thermocouple between the outer PVC insulation and the paper sheathing was still used just relocated to the underside of the cable. This was done to better check for any noticeable temperature rises in another region of the cable.

In order to examine how the presence of additional current flowing through the cable may affect the temperature of the cable, thermocouple measurements were also taken for the

experiments with a load at 200°C as was described earlier. The thermocouple was located on the underside of the cable.

2.3 Insulation Component Tests

2.3.1 Resistance Drop Testing

As previously mentioned, besides the copper wire, there are four components (paper sheathing is used in two locations) that make up the typical residential 14 AWG electric cable. These components are: inner wire PVC insulation (around the line and neutral wire), nylon coating around the inner PVC insulation, paper sheathing for the ground wire, outer cable PVC insulation, and additional paper sheathing. The individual components of the cable insulation were tested at 230°C temperature profile in order to determine when the resistance drops for each individual component. These tests were performed in order to explore the role of the resistance of each insulation component in the arcing event. The set up consisted of two small metal plates being on either side of the sample. A probe measuring resistance was placed on each plate in order to measure the resistance between the plates with an insulation component placed between them. The resistance was recorded over the time of the thermal exposure to the samples. As was the case with the cable tests, resistance measurements were recorded with only a very minimal voltage applied to the samples from the measurement device. Figure 7 shows the setup of the insulation component testing. Figure 8 illustrates how the insulation components appear when separated from the cable and each other.

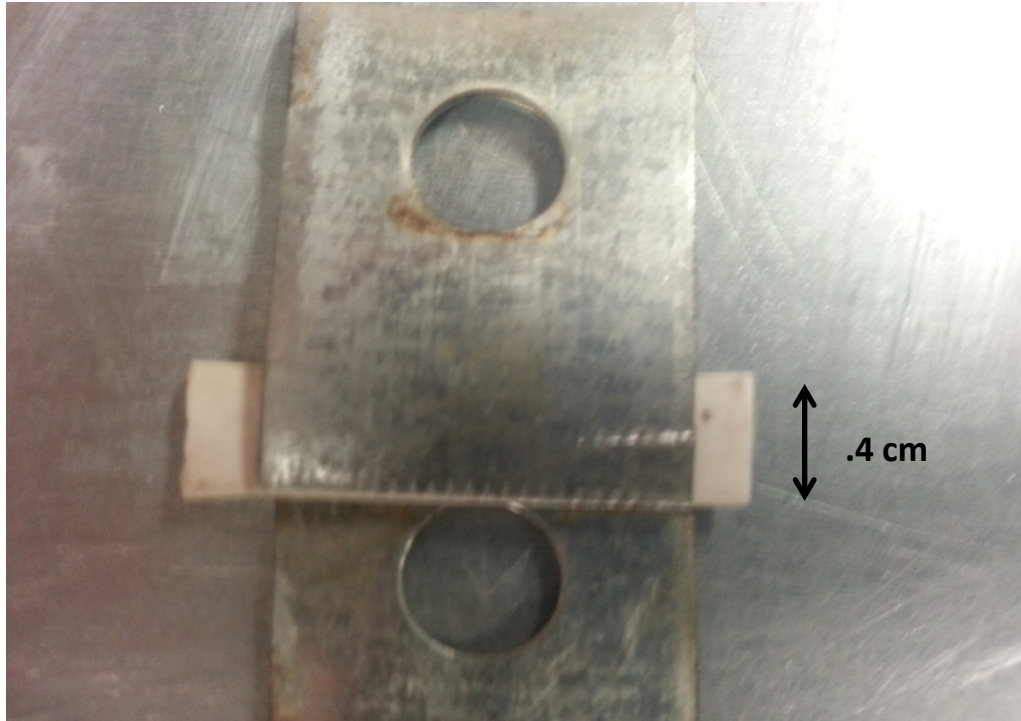


Figure 7: Insulation Component Test Set Up

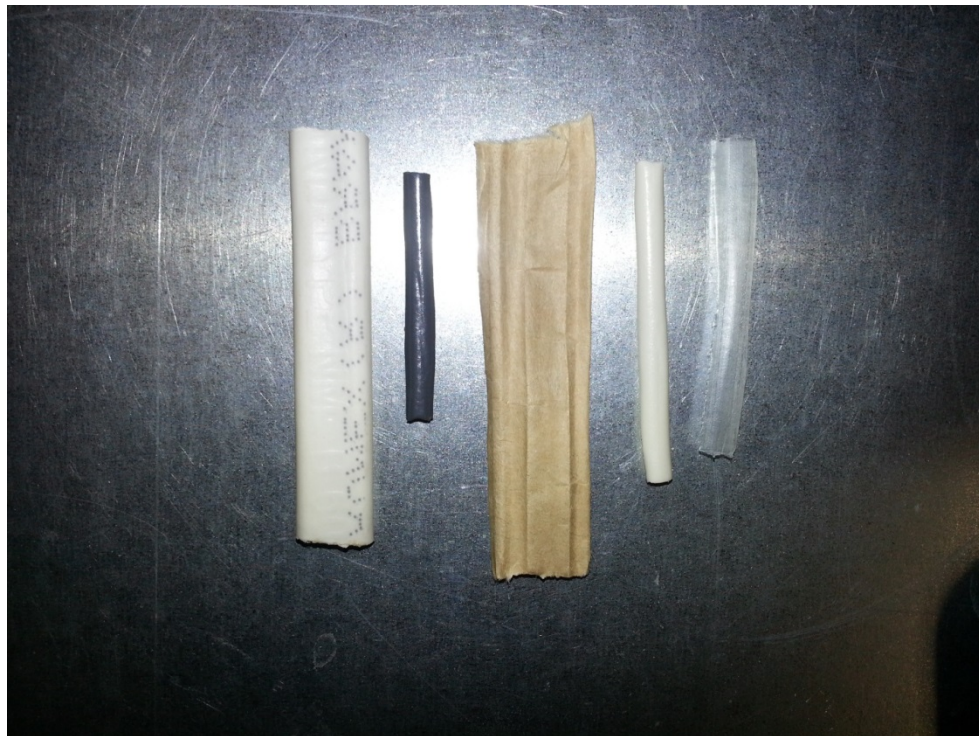


Figure 8: Cable Insulation Components

2.3.2 Energized Tests

After completion of the resistance drop testing for the individual insulation components as well as the PVC-Paper combination testing, energized testing was instrumented for the same style of component testing with the 230°C temperature profile. For this set of experiments, the same experimental set up was used except now one side of the sample was energized while the other side was not. Simply, the circuit was open due to the presence of the insulation component(s) between the two conductors. After thermal degradation, arcing events occurred across the insulation components for several cases.

2.3.3 Ground Sheathing Removed Testing

After conducting the previous experiments on the entire cable and on each of the individual insulation components, the presence of the ground wire paper sheathing proved to be an important component in prohibiting an electrical arc. Therefore, in order to greater substantiate the conjecture that the paper sheathing plays an important role in inhibiting the formation of an arc, the paper sheathing was removed from a portion of the cable. To remove part of the paper sheathing surrounding the ground wire, the outer PVC insulation and the outer paper sheathing was slightly penetrated along several inches of the cable. The ground wire paper sheathing was then cut and removed from around the ground wire. The outer PVC and paper insulation were then wrapped and secured back around the wires and the other pieces of insulation. The standard experimental cable set up was used and the cable was subjected to the 230°C temperature profile in the oven as shown in Figure 3. The region in which the sheathing was removed was varied between tests.

2.4 Insulation Component Mass Loss Analysis (TGA)

In order to better understand the thermal degradation of each of the insulation components, mass loss analysis was performed on each component. This was done using an instrument capable of thermogravimetric analysis (TGA) [14]. The microgram scale samples were exposed to a uniform heating rate of — in a nitrogen filled environment. Nitrogen was used to continuously purge the chamber. The mass of the samples were recorded over time; from this, mass and mass loss rate profiles were developed.

2.5 Modeling Approach

After capturing the mass loss rate data from the TGA apparatus testing for each of the four insulation components, a numerical pyrolysis model, was used to analyze the TGA data. ThermaKin was developed at the Federal Aviation Administration (FAA) and is a one-dimensional model that solves energy and mass conservation equations to predict material behavior experiencing thermal decomposition [15,16,17]. ThermaKin is capable of describing energy transport, chemical reactions, transport of gases, charring, and intumescent behavior of materials under thermal conditions. The model solves radiative and conductive energy transfer in conjunction with simplified thermal degradation chemistry and describes the transport of gases into the condensed phase. As a result, ThermaKin is capable of describing changes in mass over time for materials exposed to thermal conditions [16]. The ability to describe changes in mass over time allowed for the mass loss rates to be modeled by using an iterative approach to find the correct Arrhenius parameters. The benefit of ThermaKin is in its ability to be used for a wide range of materials. It was assumed that no air gaps existed within the materials and that no

ignition occurred. In summary, the model is used to provide a “parametric description of the kinetics of polymer degradation” [14].

For the purposes of this study, ThermaKin was used to model char formation under thermal conditions for each of the four insulation components. A similar approach was used in previous work on the thermal decomposition of PVC as it relates to arc failure [15]. In the previous study, generic properties of PVC were used and inputted into the model, but in this study the parameters of the specific PVC used in the cables were used. First, the model was used to mimic the conditions present of the TGA experiments. The same temperature program (10°C/min.) was prescribed and a thermally thin assumption was made in the model. This is another key difference from modeling work performed on the arc failure of electrical cables [15]. From this, an iterative approach was used to determine the Arrhenius parameters for each component. These determined values can be found in the Modeling Results section. The results of this fitting and iterative approach are shown in the mass loss data comparisons in Modeling Results section as well. For the PVC insulation components, a first-order reaction scheme was assumed when modeling the mass loss rate (The second peak in mass loss rate was ignored in the model). This assumption was made based upon the hypothesis that at the time to arc failure, the PVC would not be far enough along in the thermal decomposition process for this region to be considered. This hypothesis would later be proved correct. This can be seen in the critical degree of degradation values and the mass profiles in the Modeling Results section.

After fitting the Arrhenius parameters to the TGA data, ThermaKin was used to model the conditions of the energized, non-loaded cables exposed to the three temperature profiles. The mass data for each insulation component was tracked up until the average time to arc failure for each energized, unloaded test at each temperature profile. From this, a critical degree of

degradation of insulation components was determined to exist for arc failure to occur. This is explained in detail in the Modeling Results section.

The material in question in the model is separated into several components that are able to react physically and chemically.

3 RESULTS

3.1 Cable Tests

3.1.1 Cable Resistance Tests

The data in Figure 9 is an example of a cable resistance drop test at 230°C and is reported as an inverse resistance normalized by the length of the cable. Table 1 reports the average time to a measurable resistance between the wires as well as two standard deviations of the mean. The criterion for failure (time to resistance drop) was determined to be the point at which the first increase in the inverse normalized resistance was observed. This was determined by observing all full cable resistance drop tests and determined to be $2E-7 (\Omega m)^{-1}$. For all of the tests, this criterion for a time to resistance drop fits well. The average time failure across all tests was 72 minutes, as displayed in Table 1.

Table 1: 230°C Average Time to Resistance Drop

230°C Time To Resistance Drop (min., mean \pm 2 standard deviations of the mean)	72 +9
Failure Criteria $(\Omega m)^{-1}$	2E-7

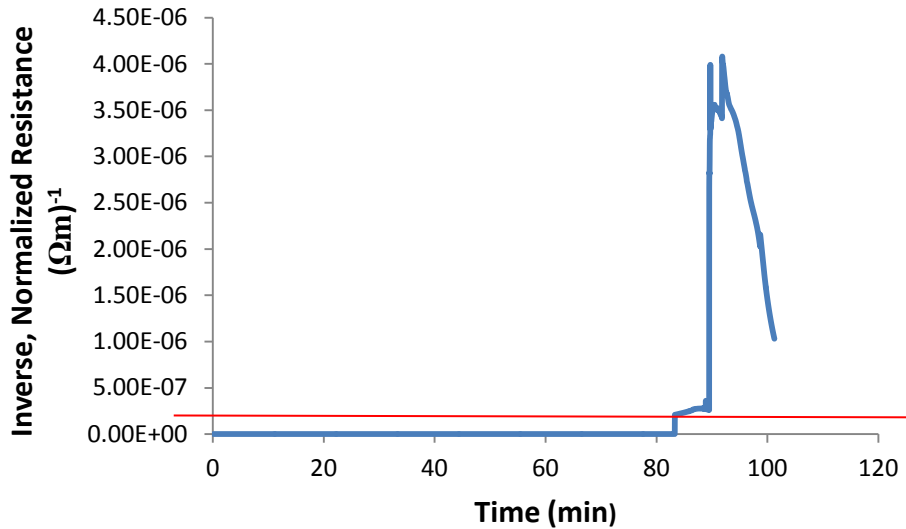


Figure 9: 230°C Inverse Normalized Resistance

3.1.2 Cable Deterioration Observations

As the cable thermally degraded, several noticeable events occurred. The PVC insulation on the outside of the cable started to smoke and began to change colors. Initially, the outside cable insulation is white, but over time it progressed to a brown color and then eventually to black. During the discoloration of the PVC cable insulation, bubbling of the PVC occurred. Once the insulation had become completely black, the PVC insulation also began to crack. At this point, the visible volatile gases were no longer produced and emitted from the material. At 230°C, the cable began to change colors after approximately 40 minutes and the very onset of bubbling and cracking occurred at approximately 80 minutes from the start; this includes the oven warm-up period of about 6°C/min. After the cable has been cooled and inspected, it can be found that the inner PVC wire insulation undergoes the same transition as the outer PVC insulation. Figure 10 shows the discoloration of the outer PVC cable insulation over time. The timeline for this transformation is dependent on the thermal conditions the cable is exposed to.

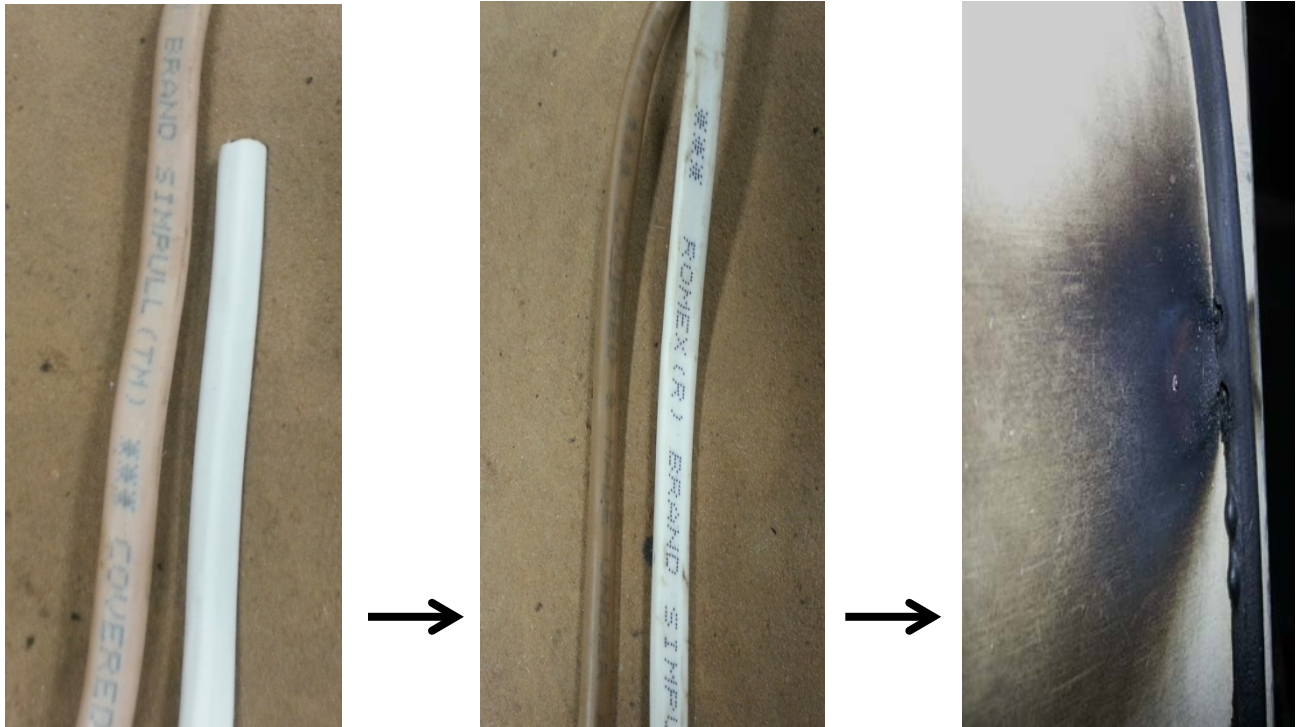


Figure 10: General Progression of the Cable Degradation Process at 230°C (40 minutes -> 65 minutes -> 125 minutes)

3.1.3 Energized, Unloaded Tests

The time to arc failure was recorded at the first visual sign of arcing event (sparking). Many times this coincided with a blown fuse in the circuit, but occasionally several short, sputtering arcing events occurred before the fuse in the circuit blew. Figure 11 shows an example of a cable post-electric arc event. The cable has undergone significant charring and as result of the arc event, molten copper was ejected from the side of the cable in the form of sparks. In the figure, ruptures in the side of the cable are obvious. A small piece of solidified molten copper is highlighted in the photo and additional photos can be found in the Appendix.

Energized, unloaded testing of the cable was performed at 200°C, 210°C, and 230°C; the times to arc failure are given in Table 2. The average time to resistance drop at the 230°C

temperature profile can be compared to the average time to arc failure for the energized, unloaded 230°C tests. Table 2 shows the time comparison and it can be seen that the resistance drop was recorded prior to the arc failure. This was expected and provides evidence that the cable, as a whole compound, is in fact deteriorating electrically prior to the occurrence of an electric arc. It is important to note that the resistance drop measurements were taken with a non-energized and non-loaded cable. The presence of an applied voltage and current (other than that of the measuring device) may affect the time to resistance drop observations under these conditions. Figure 12 displays the average time to arc failure and the two standard deviations of the mean associated with each temperature tested.



Figure 11: Cable Arc Aftermath

Table 2: Energized, Unloaded Time to Arc Failure

Temperature (7 tests)	Time to Arc Failure (min., mean \pm 2 standard deviations of the mean)
200° C	498.5 \pm 27 (\approx 8 hrs. 20 min)
210° C	243 \pm 7 (\approx 4 hrs.)
230° C	108 \pm 20 (\approx 1 hr. 48 min.) Res. Drop – 72 +/- 9 min.

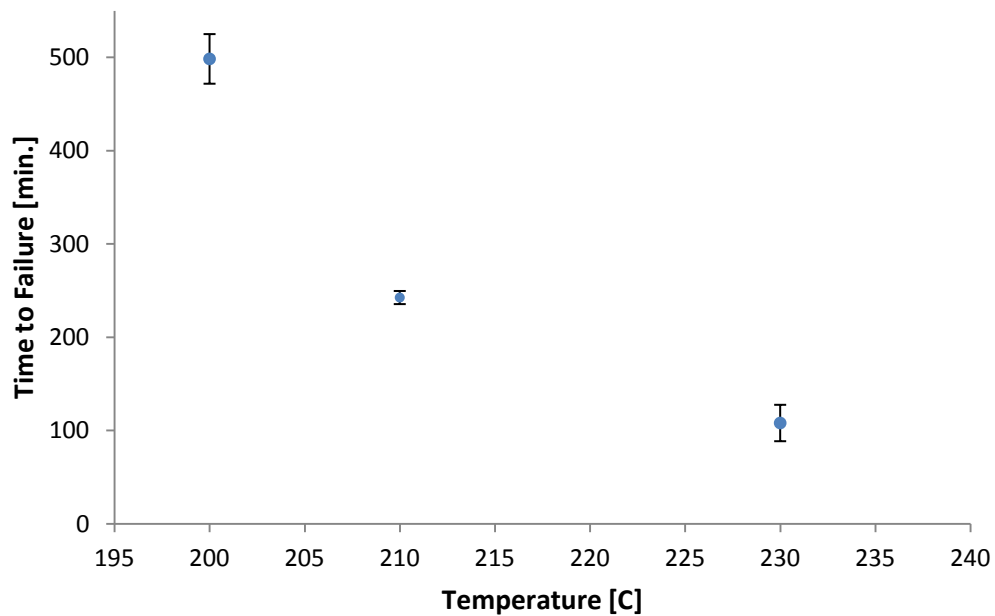


Figure 12: Energized, Unloaded Cable Time to Arc Failure

Figure 13 shows the current signature in the last moments of one energized, unloaded cable test at 230°C. The current remains at 0 Amps leading up to an arcing event at which point the magnitude of the current reaches up to 250 Amps during the arcing event. After several cycles, the immense amount of current caused the 20 Amp fuse to blow and open the circuit, therefore ending the test.

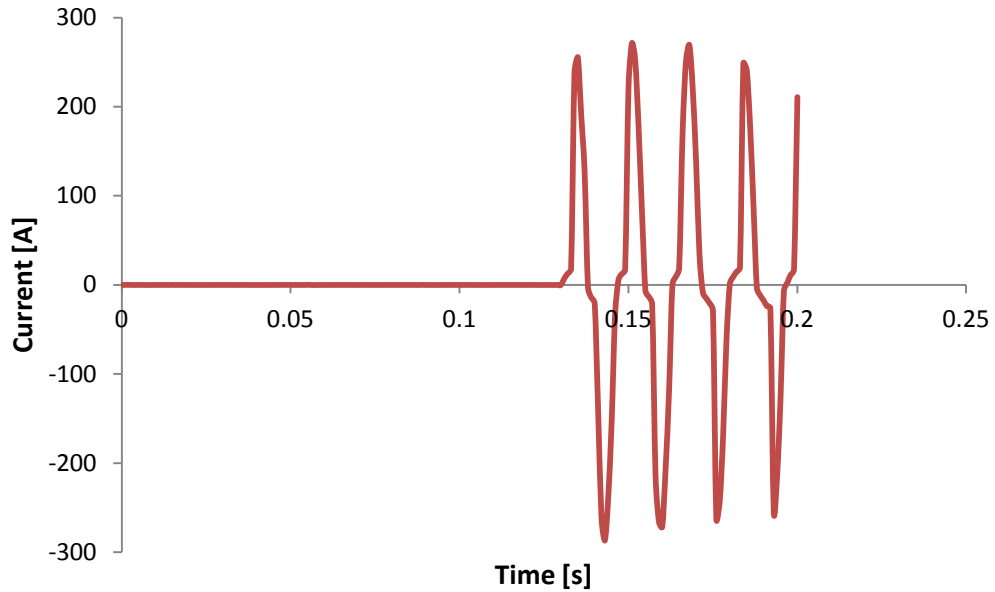


Figure 13: Energized, Unloaded Cable Arc Current Signature

3.1.4 Arcing Observations

When the arcing event occurred, a loud humming sound erupted and sparks begin to be ejected from the cable. At this point, in most cases, the fuse will have blown and the circuit was shut down manually past the fuse. Throughout the entirety of this study, the 20 Amp fuse failed prior to activation of the 15 Amp circuit breaker. Several types of circuit breakers were experimented with throughout testing, but no circuit breaker activation occurred. The arcing event finished either when the fuse was blown or when the wires were broken due to the immense amount of energy from the event. Either way, the circuit was now open and the test concluded. The arcing event melts the copper in the wires and emits sparks in the form of molten copper. Figure 14 is a snapshot of a high speed video of an arcing event at 230° C. Additional photographs are available in the Appendix.



Figure 14: Arcing Event

3.1.5 Added Insulation Tests

The first added insulation test subjected the cable to a temperature of 65°C. This was a conservative estimate based on data by Armin Rudd and Joseph Lstiburlek on hottest attic temperatures in Las Vegas [13]. With added thick fiberglass insulation, 100% continuous loading, and a temperature representative of an attic or in wall space on one of the hottest days of the year (65°C), it was explored if the cable would exhibit electrical arc failure. After a total exposure of approximately 60 hours spread out over 7 testing days, the cable did not fail due to an electrical arc failure.

After running the set of experiments at 65°C and without experiencing any electrical arc failure, the same experiment was repeated with a new piece of cable, but this time subjected to a temperature of 100°C. The cable was once again under 100% of its rated continuous load capacity with added fiberglass insulation of top of it. After approximately 60 hours of testing

over 7 testing days, the cable once again did not exhibit electrical arcing failure. In this scenario, the temperatures measured within the cable (just under the outer PVC insulation) reached up to 115°C. This was the greatest difference between the cable and atmospheric temperatures observed in any of the testing scenarios. This shows that the added insulation does in fact have a significant effect on preventing heat from dissipating from the loaded cable; however, it is not dramatic enough to cause electrical arcing failure within a 60 hour testing scenario at 100°C atmospheric temperature.

3.1.6 Sharp Bends Tests

The results from the 200°C sharp bend tests are compared to the 200°C energized, unloaded test results in Table 3 and show that there was not a significant impact on the time to arc failure due to the sharp bending of the cable. There is an increase in time to failure for the sharp bends set up over the original set up, however this falls within two standard deviations of the mean of the time to failure of the original set up so was determined to be negligible.

Table 3: Cable Geometry Time to Failure Comparison

	Time to Failure (min. – Mean ± 2 Std. Dev. Of Mean)
200°C, Original Set Up (7 tests)	498.5 ± 27
200°C, Sharp Bends (7 tests)	523 ± 12

3.1.7 Energized, Loaded Tests

According to the National Electric Code (NEC, NFPA 70) 240.4 (D) 3 – 14 AWG copper wire shall be protected by 15 amperes circuit protection [12]. Additionally, NFPA 70 210.20 (A) requires “where a branch circuit supplies continuous loads or any combo of continuous and non-continuous loads, the rating of the overcurrent device shall not be less than the non-continuous load plus 125% of the continuous load” [12]. Therefore, since 14 AWG copper wire requires 15A circuit protection, the maximum possible continuous or non-continuous loading allowed by NFPA 70 is 12A. A 12A current represents a 100% loading for this wire and cable and was used as the first set of testing involving current. Additionally, a 150% loading (18A) was tested at 200°C as well. The time to electrical arcing failure was the sought after criteria and the results of these tests, as well as the unloaded, energized cable experimental results, are shown in Table 4 and Figure 16. In Figure 16, it is hard to distinguish, but the two standard deviations of the mean is 10 minutes for the 18 Amp test.

Table 4: 200°C Unloaded and Loaded Time to Failure Comparisons

Test Method	Time to Electrical Arcing Failure (+/- 2 Std. Dev. Of Mean in minutes)
200°C, No Current	498.5 +/-27 (\approx 8 hrs. 20 min)
200°C, 12 Amps	369.9 +/- 26.2 (\approx 6 hrs. 10 min)
200°C, 18 Amps	235.7 +/- 9.5 (\approx 4 hrs.)

Figure 15 is an example of a test performed at 200°C and a load of 12 Amps. As expected, the recorded current of 12 Amps exists leading up to the arcing event. During the arcing event, the current reaches a magnitude in excess of 200 Amps before blowing the fuse and ending the test. The lag before the fuse blows is due to the thermal lag in the device.

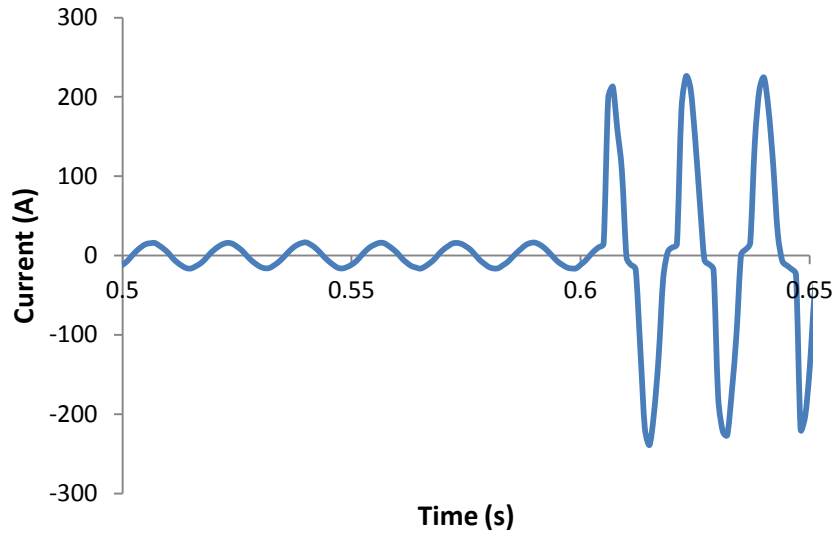


Figure 15: Energized, Loaded Cable Arc Current Signature

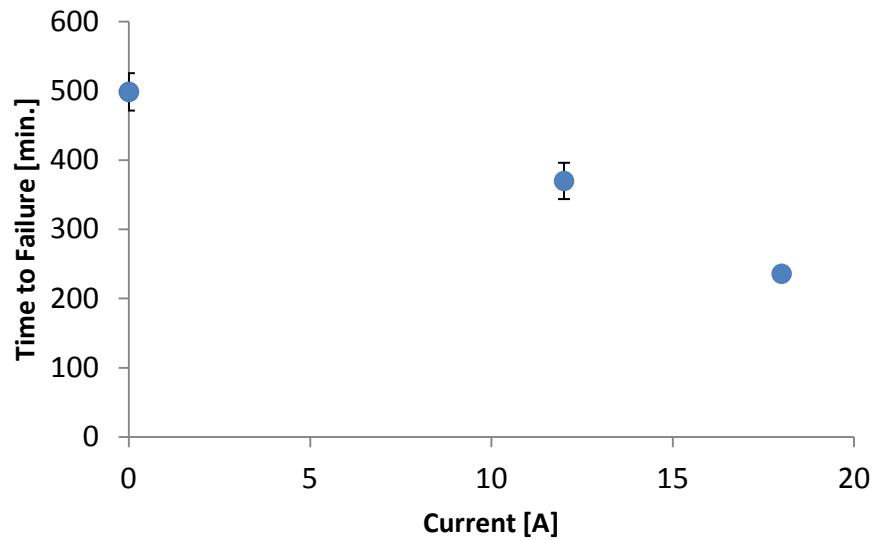


Figure 16: 200°C Time to Arc Failure Times per Load

As Table 4 and Figure 16 portray, the time to arc failure depended significantly on the current in the cable. However, temperature measurements were made inside the cable just below

the outer PVC insulation and an elevated temperature within the cable was noted. The average temperature inside the cable was found to be greater than the oven environmental temperature. This increase in temperature within the cable is another factor which may influence the time to arcing failure of the cable. The difference in temperature within the cable as compared to the atmospheric temperature of the air in the oven is due to the presence of a current within the cable. The energy from the current heats the cable to a temperature that is a few degrees higher than the air temperature in the oven. The intensity by which the temperature of the cable is warmer than the oven atmosphere depends on the amount of current flow within the cable. The increased temperatures for the energized, loaded testing scenarios will be referenced again in the Modeling Results section of this report. Table 5 shows the average steady-state internal cable temperatures in all three 200°C loaded scenarios. The average cable temperature was calculated after the cable reached the prescribed oven atmospheric temperature and up until arc failure.

Table 5: 200°C Cable Internal Temperatures

Load Scenario	No load	12 Amps	18 Amps
Cable Temperature (C)	200	202	204

3.1.8 Temperature Analysis of Cables

The temperatures reported for all scenarios are for underneath the outer PVC insulation, but not for the center of the cable. Figures 17 through 21 show the temperature measurements taken during the last thirty minutes of the energized, unloaded experiments. These temperature profiles only represent the temperature measurements in the last thirty minutes of testing leading up to the arc failure of the cable and are meant to explore a final temperature rise in the cable. The average cable temperatures reported for the each cable testing setup in other areas of this

report are different pieces of data that refer to average temperatures taken over longer periods of thermal exposure time. As is shown, temperature rises were seen in the cable on occasional tests leading up to the arc failure. For the 230°C tests in Figure 19, the temperature rise recorded in the cable can be associated with the cable still being heated by the oven, as the oven was just finishing the temperature ramp process at this point. Figures 20 and 21 show the temperature measurement results for the last thirty minutes prior to arc failure for the loaded experiments. A slightly noticeable increase in temperature in the 18 Amp loaded scenarios can be seen in comparison with the 12 Amp scenarios and the 200°C energized, unloaded tests. The dotted line indicates when the arc failure occurred.

In the temperature measurement data, some inconsistent data was recorded. It is hypothesized that localized heating within the cable does in fact occur leading up to the electric arc failure. This is why the temperatures in the final 30 minutes of each experiment were examined. However, this is not consistently seen in the temperature data. A reason for this may be due to having a single thermocouple in the cable. In order to better understand this phenomenon, it is recommended to add many more thermocouples into the cable measurement process.

A hypothesis was made that the increased temperature measurements were a result of localized heating caused by leak current in the cable as the insulation components degraded. As parts of the insulation degraded, it was hypothesized that small amounts of current were able to travel across small areas of the cable that were resistively-compromised. To explore this, the power analyzer was used to measure current in the cable for energized, non-loaded cables and for cables subjected to an 18 Amp load. When a 1000 Hz resolution was used and on a non-energized and non-loaded cable, the instrument typically recorded current measurements on the

order of .2 Amps (absolute value). This .2 Amps measurement is considered the uncertainty (or noise) of the equipment. When the measurements were conducted on the energized, unloaded cables and in the tests with an 18 Amp current, no noticeable increases outside of the previously recorded uncertainty were noted in the moments leading up to the arcing event. Additional information regarding this topic is discussed in the “Future Works” section of this report.

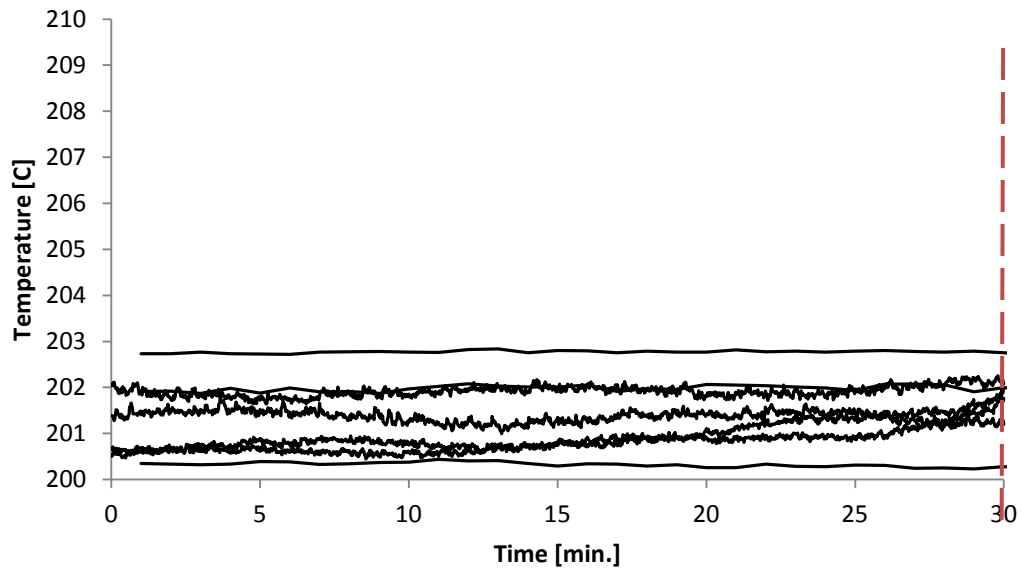


Figure 17: 200°C Energized, Unloaded Cable Temperature Rise

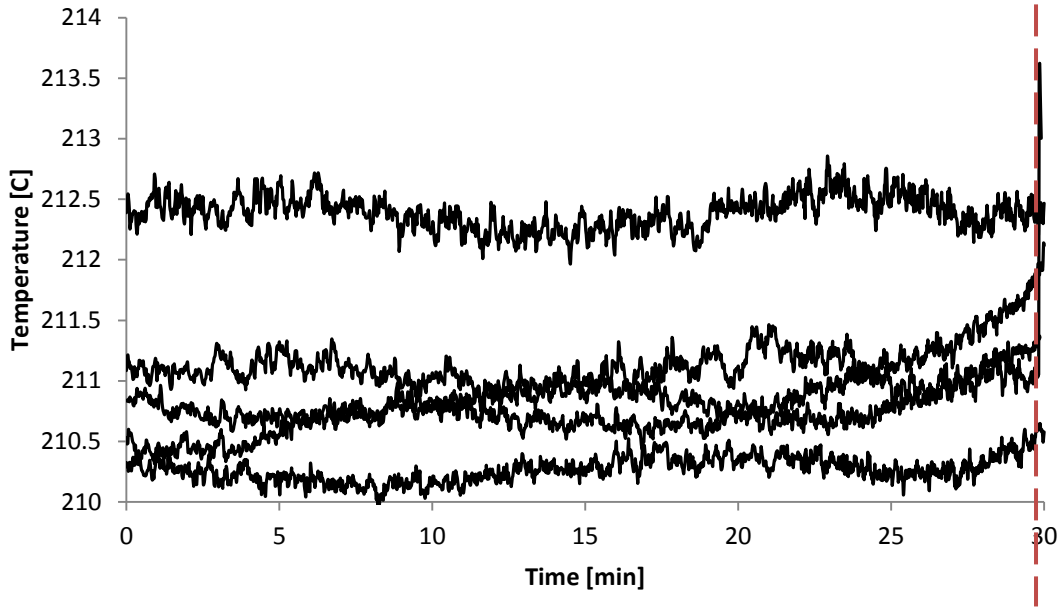


Figure 18: 210°C Energized, Unloaded Cable Temperature Rise

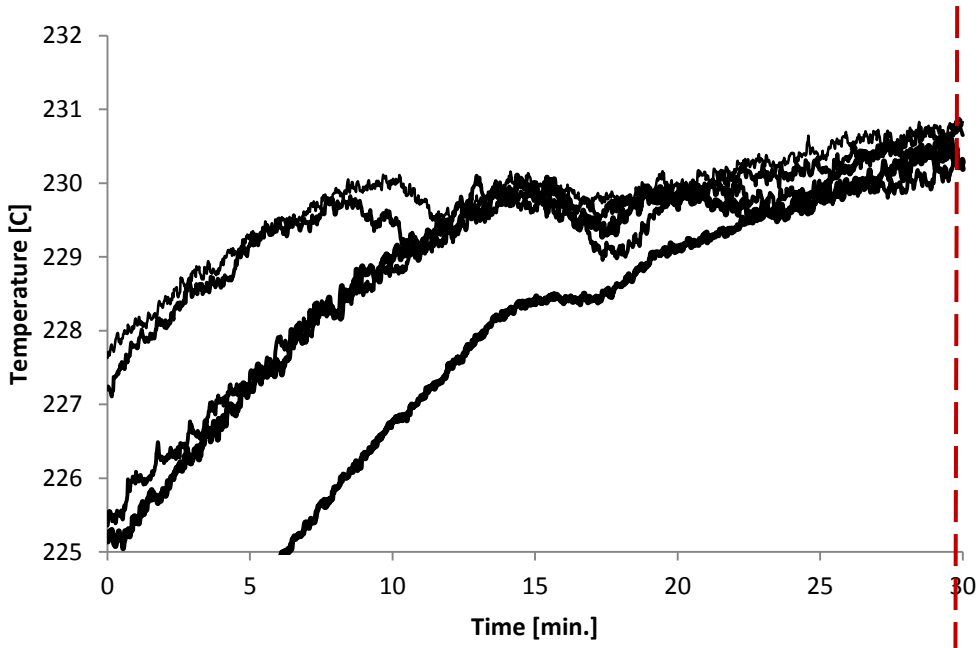


Figure 19: 230°C Energized, Unloaded Cable Temperature Rise

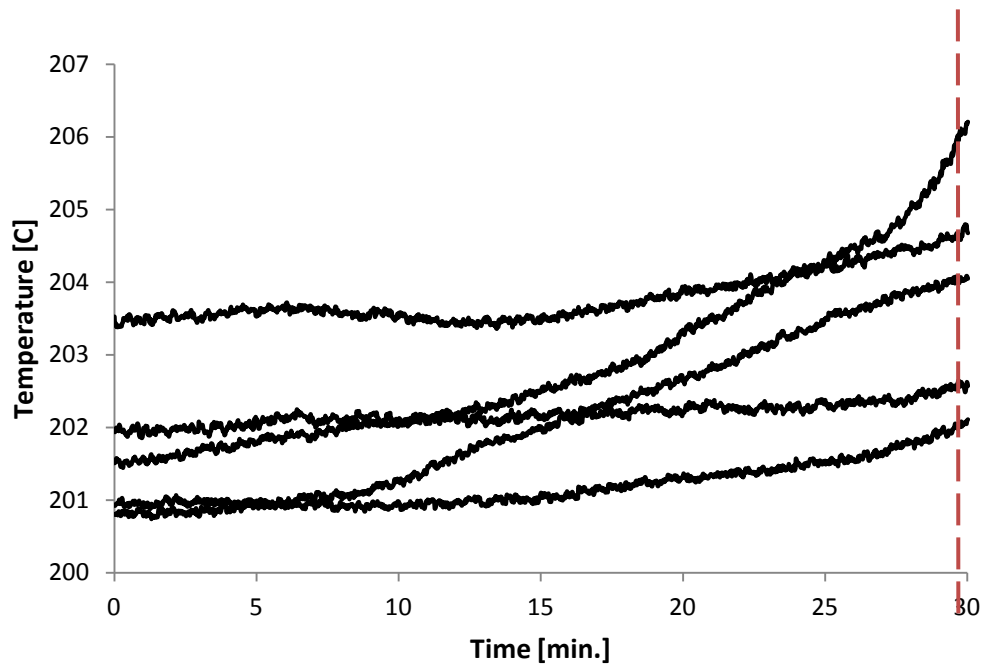


Figure 20: 200°C Energized, 12 Amp Loaded Cable Temperature Rise

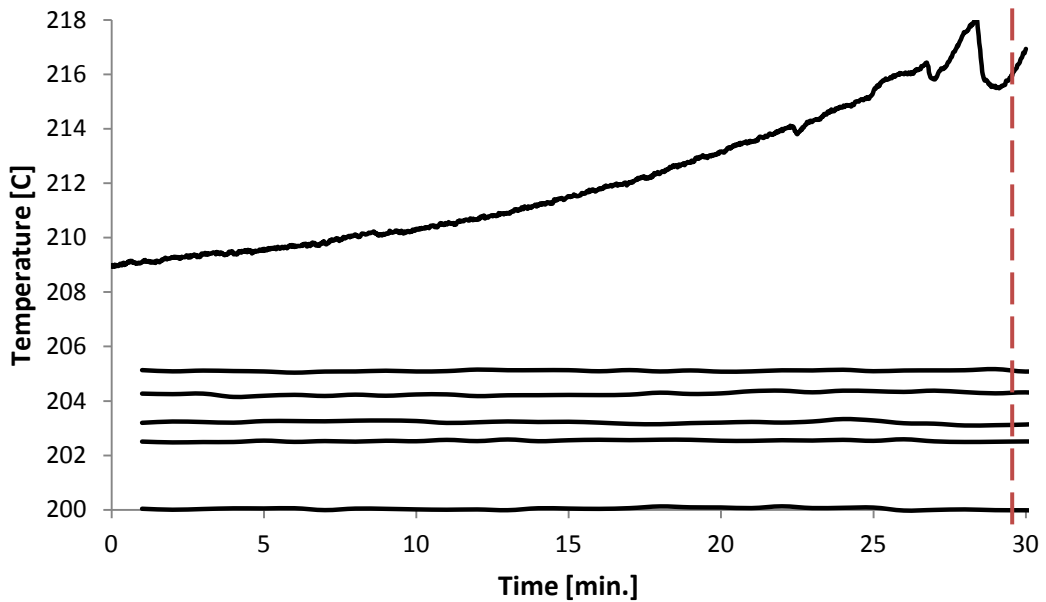


Figure 21: 200°C Energized, 18 Amp Loaded Cable Temperature Rise

3.2 Insulation Component Testing

3.2.1 Resistance Drop Testing

From the resistance drop testing for each of the insulation components, an inverse, normalized resistance was determined from the resistance measurements and the surface area of the samples used in the experiments. Therefore, the inverse, normalized resistance measurements are reported in units of $\Omega^{-1}\text{m}^{-2}$. Examples of this for the outer PVC insulation, inner PVC insulation, nylon coating, and paper sheathing are shown in Figure 22.

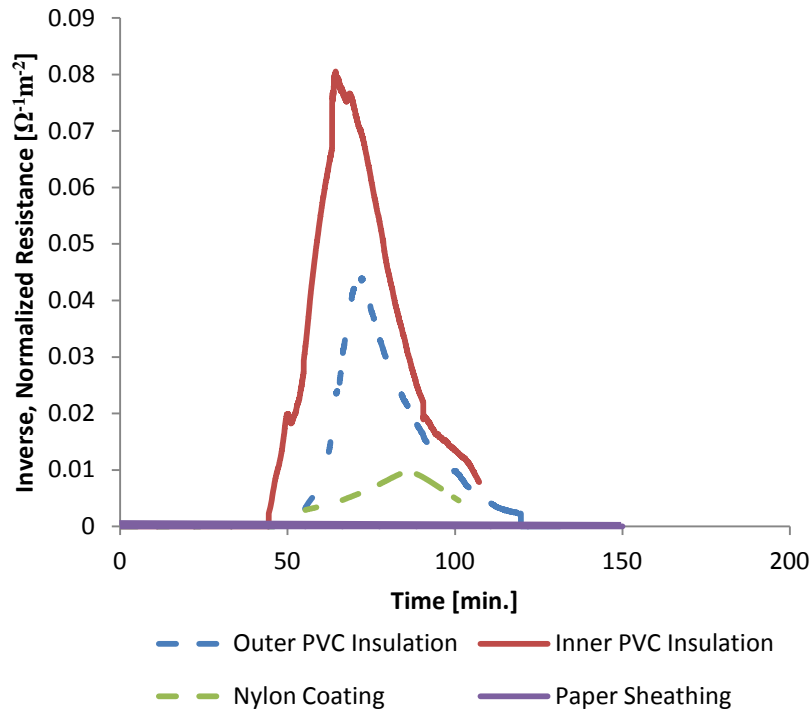


Figure 22: 230°C Insulation Component Inverse, Normalized Resistance

During the exposure, the paper sheathing did not show any measurable drop in resistance for up to 150 minutes. The times in Table 6 are noticeably less than the average time to resistance drop in the entire cable of 72 minutes that shown in Table 1.

Table 6: 230°C Component Time to Resistance Drop Tests

Insulation Component (7 tests)	Time to Resistance Drop (Min. – Mean \pm Two Std. Dev. Of Mean)
Outer PVC	50 \pm 6
Inner PVC	42 \pm 3
Nylon Coating	49 \pm 6
Paper	> 150

As previously mentioned, no resistance drop was seen in the paper sheathing. As a result, the interaction between the PVC insulation and the paper sheathing was explored. To do this, PVC insulation samples were placed flat against the paper sample on both sides and time to resistance drop tests were performed at 230°C (the same experimentation was explored for a nylon-paper combination). Figure 23 portrays a magnified set up on the PVC-Paper combination resistance drop test. Additional photos of this setup are available in the Appendix. For the outer PVC insulation-paper combination tests, a resistance drop was observed in 39% of tests (14/36 tests) and for the nylon-paper combination tests, no resistance drop was observed. The results of the PVC-paper and Nylon-paper resistance drop test can be seen in Table 7.

Table 7: 230°C Component Time to Resistance Drop Tests w/ Combination

Insulation Component (7 tests)	Time to Resistance Drop (Min. – Mean \pm Two Std. Dev. Of Mean)
PVC-Paper Combination	86 \pm 7
Nylon-Paper Combination	>150



Figure 23: PVC-Paper Component Post Resistance Testing (Top Plate Removed for Picture)

3.2.2 Energized Tests

Each of the insulation component was put into the same set up as for the insulation component resistance drop tests. However, this time one of the two metal plates was energized. For the outer PVC, inner PVC, and nylon components, arcing occurred after being exposed to 230°C heating profile. However, no arcing event occurred across the paper sheathing or across the PVC-Paper combination (up to 150 minutes). While an effort was made to introduce as much PVC insulation as reasonably possible in the PVC-Paper combination testing, it is hypothesized that there was not a significant enough amount of PVC in the PVC-Paper combination tests to cause the paper to degrade enough to allow an arc to occur. In each scenario where arc failure occurred, the average time to failure was observed to occur prior to the

average time to arc failure in the full cable experiments. Results from the resistance drop testing and the energized testing are shown in Table 8.

Table 8: 230°C Component Time to Resistance Drop, Arc Failure Comparisons

Insulation Component (7 tests)	Time to Resistance Drop (Min. – Mean \pm Two Std. Dev. Of Mean)	Time to Arc Failure
Outer PVC	50 \pm 6	61 \pm 9
Inner PVC	42 \pm 3	54 \pm 12
Nylon	49 \pm 6	75 \pm 3
Paper	> 150	> 150
PVC-Paper Combination	86 \pm 7	> 150

3.2.3 Ground Paper Sheathing Removed Tests

From the insulation component resistance drop and electric arcing tests, it was found that the paper alone was not able to resistively-compromise enough for a measurable resistance drop to exist nor for an electric arc to occur across the paper under the given thermal conditions. However, the entire cable exhibited measurable resistance drops between the hot and ground wires as well as electrical arcing events between the conductors under the given thermal conditions.

The time to failure of these experiments and the location of the arc event were the main data points of interest in these experiments. In 6/7 of the tests performed, the electrical arc occurred in the region of the cable where the ground wire paper sheathing was removed. The data involving the failure locations at the region without paper ground sheathing and the data in Table 9 shows that without the presence of the paper ground sheathing, the electrical arc forms faster and in the region lacking the paper sheathing. The results of this set of testing highlight the impact of the ground paper sheathing in preventing or delaying arc failure.

Table 9: Removed Ground Paper Sheathing Time to Arc Failure

Test Method	Time to Failure (min. – Mean \pm Two Std. Dev. of Mean)
230°C, Standard Testing	108 \pm 20
230°C, Removed Paper Sheathing	81 \pm 12

3.4 Insulation Component Mass Loss Analysis (TGA)

Each of the cable insulation components was exposed to a uniform heating rate of 10— in the TGA apparatus as was previously described. The chamber in the TGA apparatus was purged with Nitrogen. This was done in order to mimic the anaerobic conditions that would exist internally in the cable prior to an arcing event occurring. The charring polymers (PVC insulation components) exhibited two peaks in mass loss rate, while the Nylon and Paper did not. These results were to be expected based on prior research performed on the subject of the degradation of polymers [14]. Analysis was performed on the outer PVC insulation in air as well and there was not a difference in recorded mass loss rate data. The mass loss profiles for each component in the TGA apparatus are shown in Figures 24 through 31. These mass loss profiles will be used in the Modeling Results section to calibrate a model for predicting electrical arc failure.

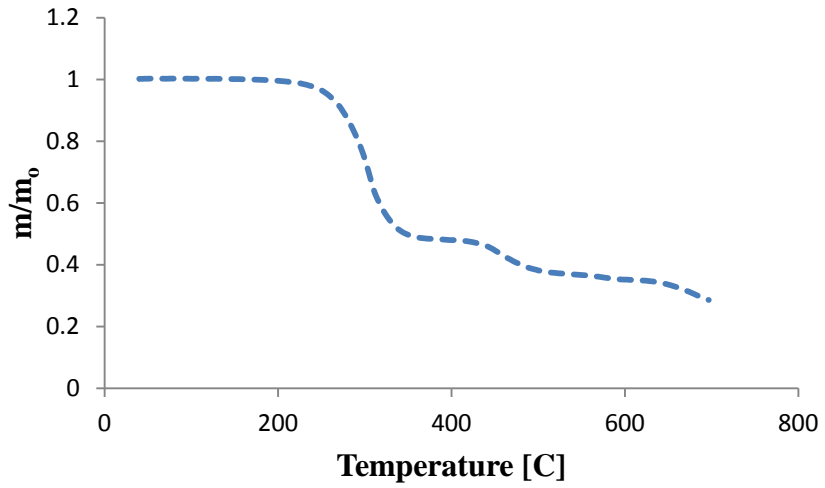


Figure 24: Outer PVC Mass - TGA

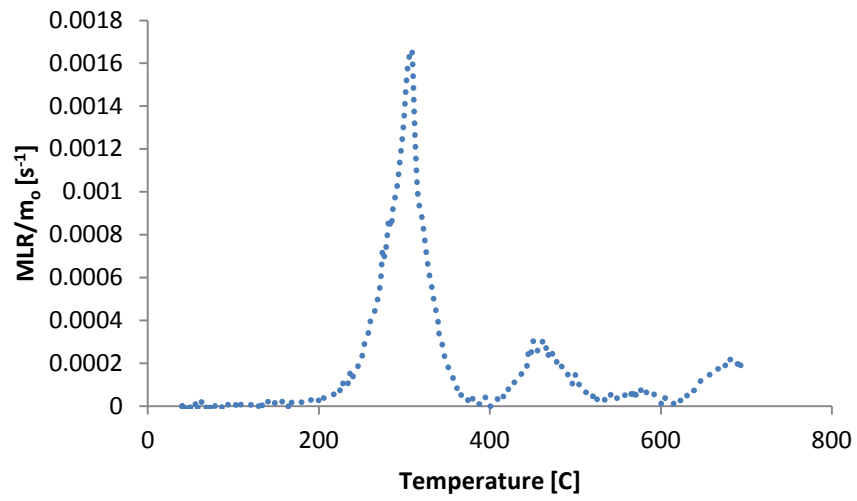


Figure 25: Outer PVC Mass Loss Rate - TGA

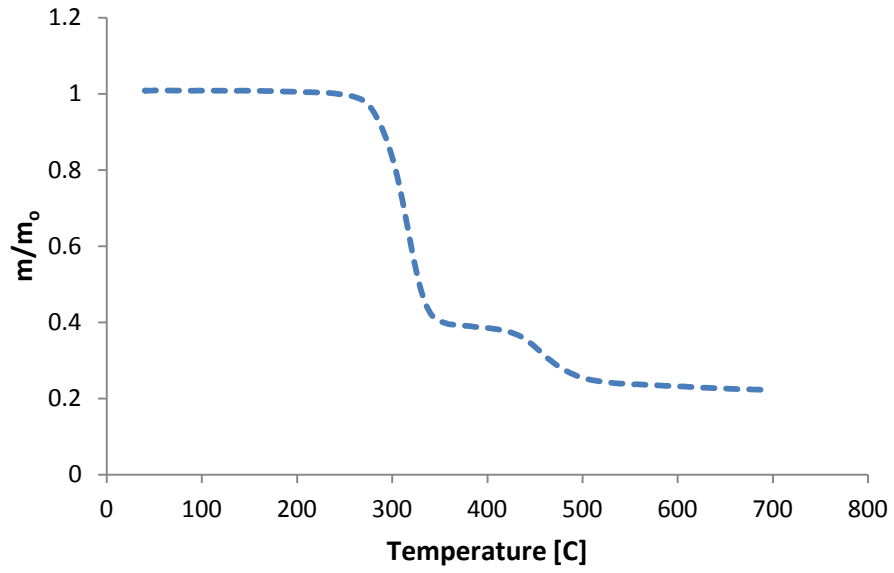


Figure 26: Inner PVC Mass - TGA

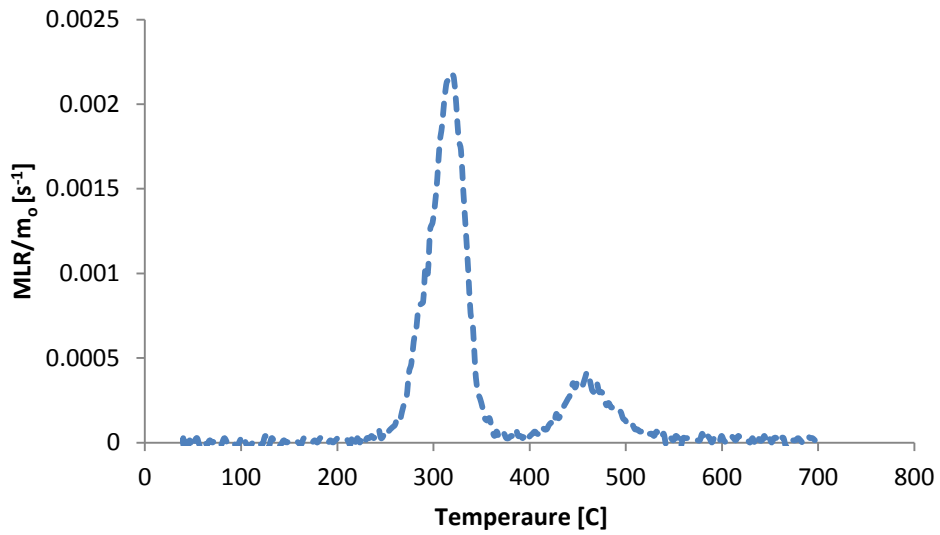


Figure 27: Inner PVC Mass Loss Rate - TGA

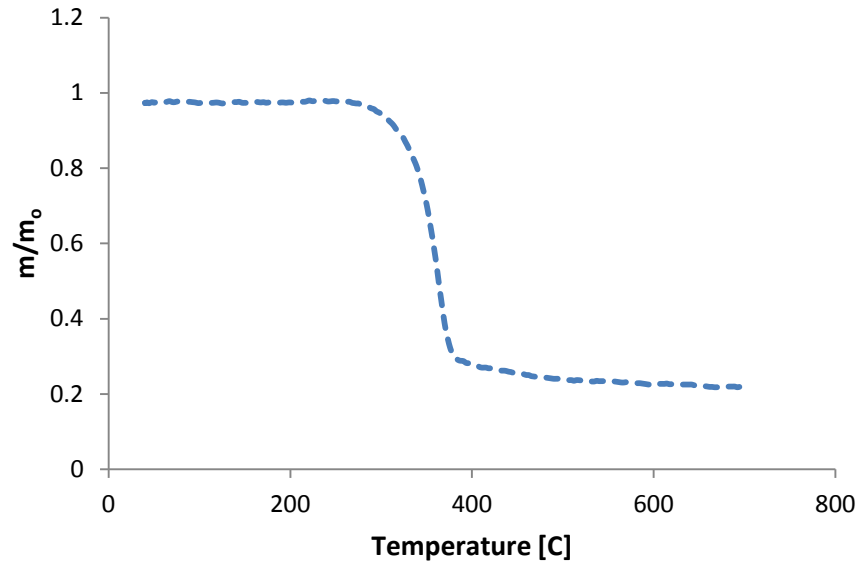


Figure 28: Paper Mass - TGA

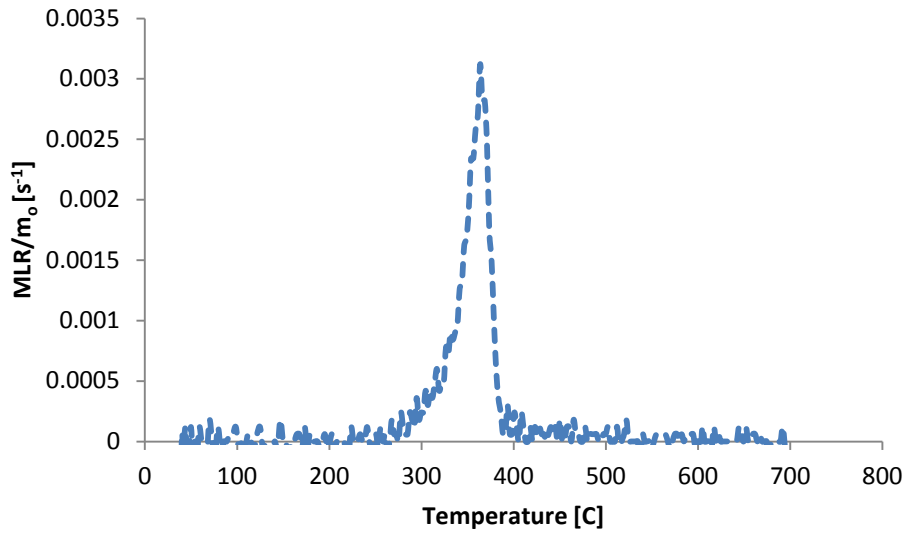


Figure 29: Paper Mass Loss Rate - TGA

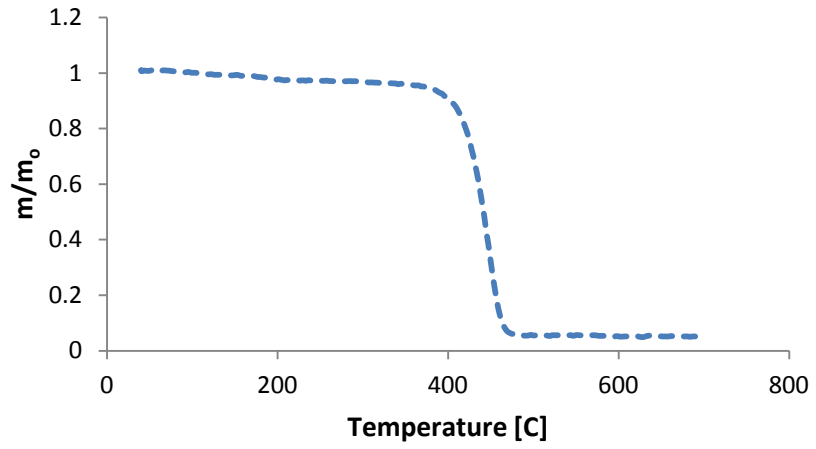


Figure 30: Nylon Mass - TGA

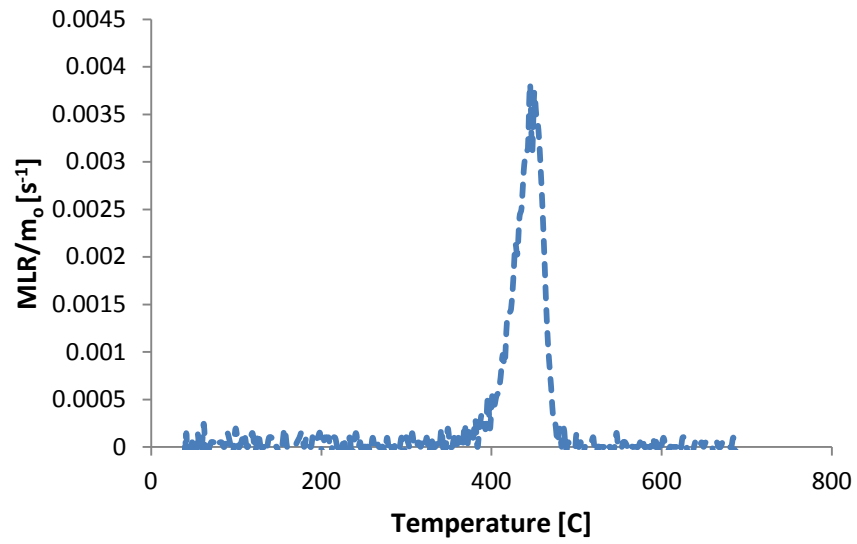


Figure 31: Nylon Mass Loss Rate - TGA

4 MODELING RESULTS

After compiling the information from the TGA results and using the methods describing in section 2.5, a model was developed to determine the Arrhenius parameters for the insulation components. The experimental results were used to calibrate a model that will be used to predict time to arc failure under known thermal conditions. Table 10 shows the Arrhenius parameters that were determined in a iterative process when modeling the mass loss data from the TGA testing method for each insulation component. Figures 32 through 39 show the TGA results as compared to the modeled data.

Table 10: Insulation Component Arrhenius parameters

	A (s ⁻¹)	E (kJ mol ⁻¹)
Outer PVC	7.98 x 10 ¹⁰	145
Inner PVC	2.62 x 10 ¹¹	152
Nylon	2.30 x 10 ¹⁸	281
Paper	2.40 x 10 ¹⁵	212

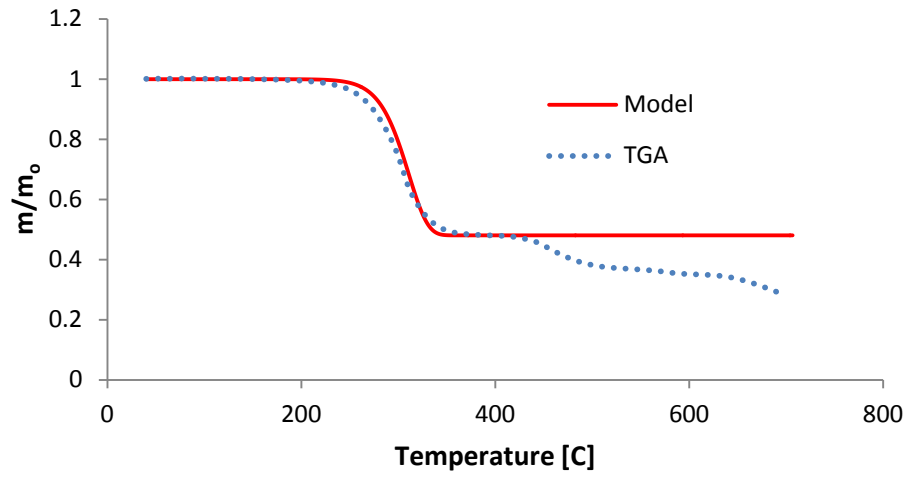


Figure 32: Outer PVC Model Mass Fit

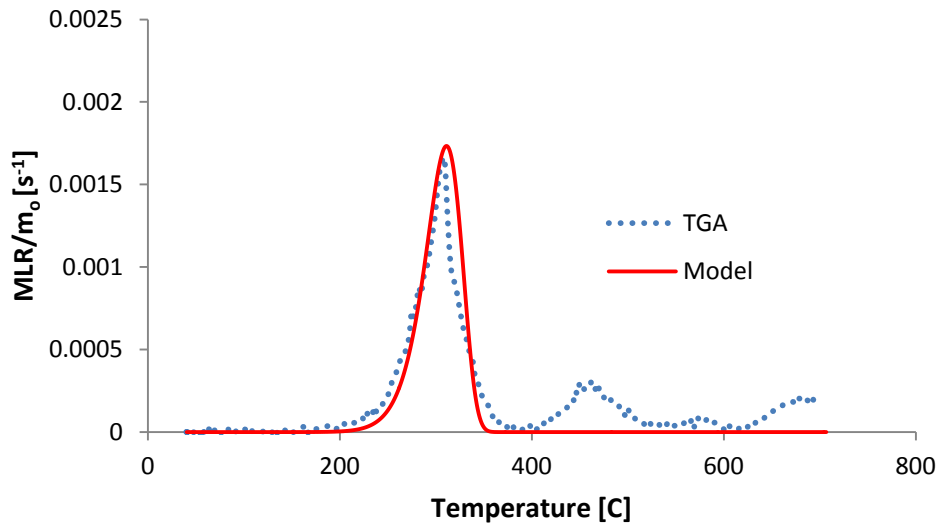


Figure 33: Outer PVC Model Mass Loss Rate Fit

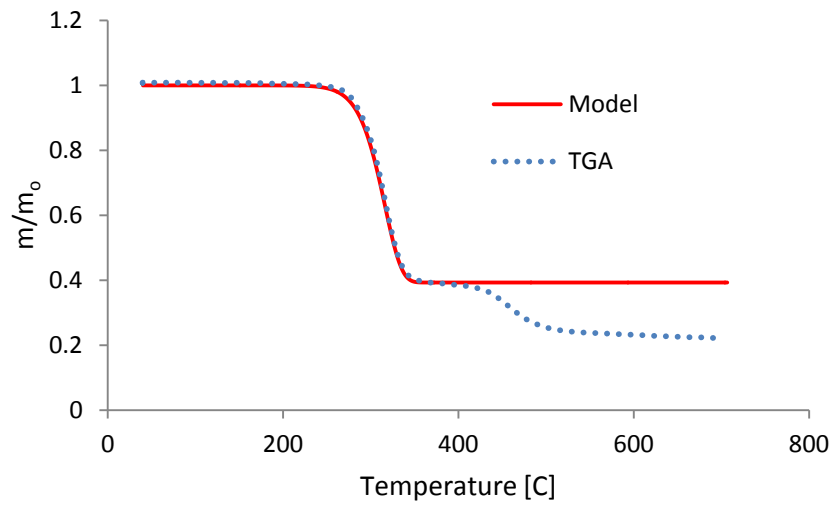


Figure 34: Inner PVC Model Mass Fit

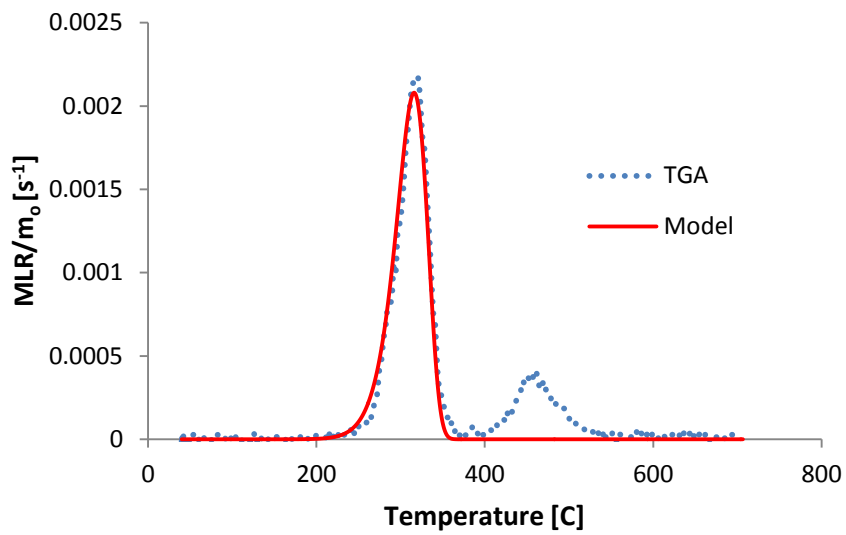


Figure 35: Inner PVC Model Mass Loss Rate Fit

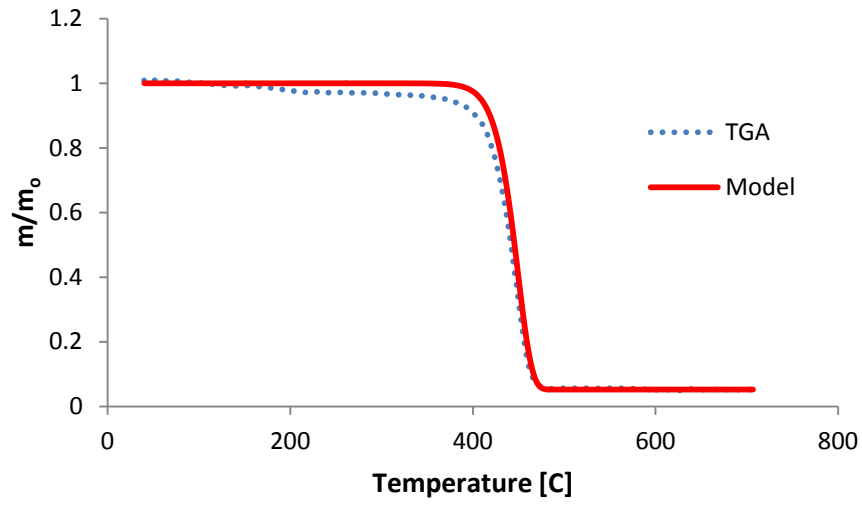


Figure 36: Nylon Model Mass Fit

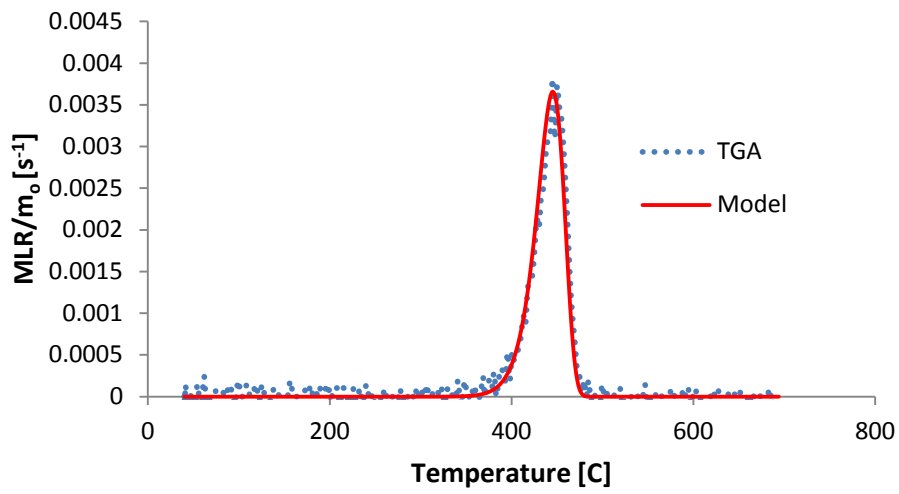


Figure 37: Nylon Model Mass Loss Rate Fit

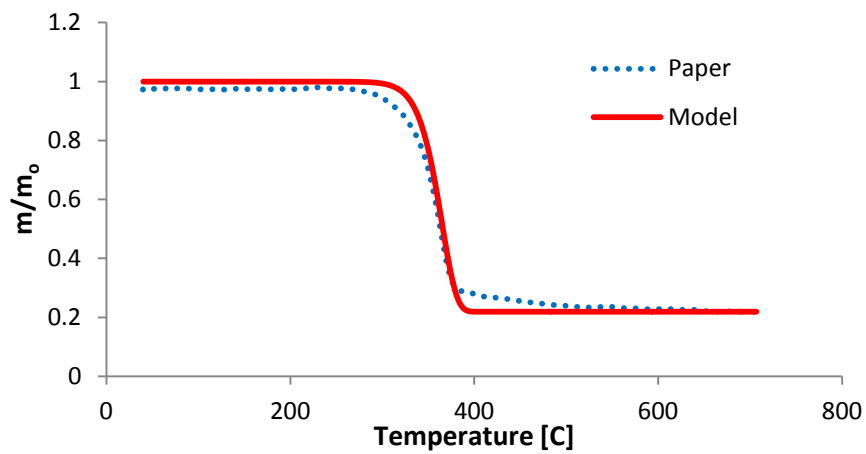


Figure 38: Paper Model Mass Fit

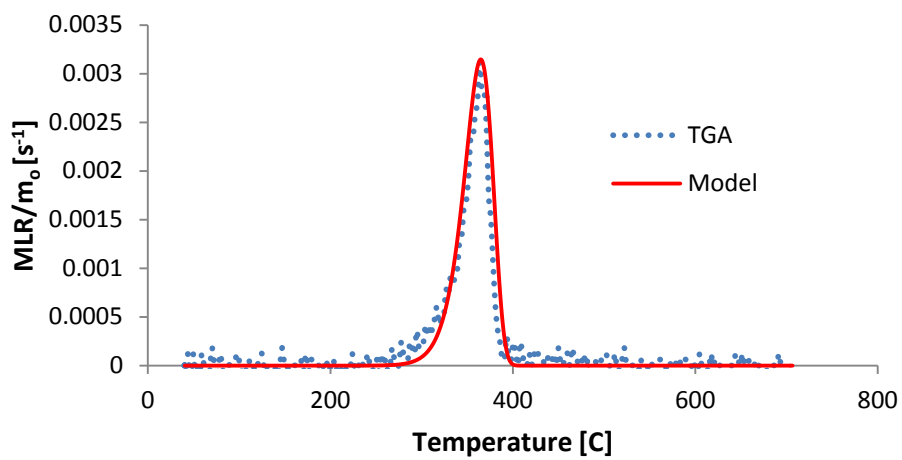


Figure 39: Paper Model Mass Loss Rate Fit

The Arrhenius parameters that were determined based on the results from the TGA testing were now used in an additional modeling approach. These parameters were then used to model the state of each insulation component based on the conditions within the testing oven. Simulations were conducted for each insulation component at each of the three main testing temperatures (200°C, 210°C, 230°C). The temperature profile of the oven tests were prescribed in the model and the end of the simulation was set to be the experimental average time to arcing failure for full cable tests at each respective testing temperature. For example, ThermaKin simulations used to model the 200°C oven temperature experiments had a prescribed temperature program to match that of the 200°C oven temperature profile and ended after 498.5 minutes for each insulation component. 498.5 minutes is the average time to arc failure for the 200°C energized, unloaded cable experiments; the average time to arc failure for these experiments can be found in Table 2. The energized, unloaded experimental time to failures were then used to begin the development of a predictive model. At the end of the oven-replicating simulations, the mass concentration of char and virgin solid of each insulation component was noted. The mass of the gas given off from the material during thermal decomposition had a negligible effect on the overall mass of the material because it was expected to leave the material. The mass concentration findings are described as a critical degree of degradation that exists at the time of arc failure and are listed in Table 11. The critical degrees of degradation calculated to exist at the average time to arc failure for each temperature profile in the model produced particularly consistent results. The consistency of these results brings confidence to the inputs and determined failure criteria for electrical arc failure. The definition of critical degree of degradation is listed below.

Table 11: Component Degrees of Degradation at Arc Failure

	200°C	210°C	230°C
Outer PVC	.89	.87	.89
Inner PVC	.95	.94	.94
Nylon	1.0	1.0	1.0
Paper	1.0	1.0	1.0

As expected, the nylon coating and paper sheathing were not predicted by the model to exhibit any mass loss during the modeled oven scenarios. This shows that the thermal degradation of the PVC components may be the critical component to the process leading up to the arcing event of the cable. As seen in Table 7, it was found that a resistance drop can occur across the combination of the PVC and paper insulation components. It is hypothesized that the reaction between the hydrogen chloride gas that is released from the PVC insulation at high temperatures and the nylon and paper components causes there to be a path of compromised resistance across the insulation components [18]. HCL is an incompatible substance with organic materials, such as paper, due to its acidic nature [19].

Therefore, the degree of degradation of the PVC components is referred to as the critical degree of degradation at which arc failure can be expected or predicted. The prior assumption to

ignore the second peak in the mass loss rates for the PVC components is proved to be valid. As can be seen in the inner and outer PVC insulation component mass loss rates in Figures 32 and 37, the critical degree of degradation occurs prior to when the PVC components experience the second peak in mass loss rate. From this degree of degradation and the model described above with the previously determined Arrhenius parameters for each insulation component, times to arcing failure at temperatures other than those tested were able to be predicted. For modeling cable time to arc failures at temperatures other than those tested, the critical degree of degradation of the outer PVC insulation was used. The outer PVC insulation was chosen as the critical component when modeling because it is the primary producer of HCl. This is due to the vast abundance of it in the cable structure. The value used for this was . This modeling approach followed this procedure:

- The temperature program was specified and the outer PVC insulation information was prescribed
- The simulation was run for an extended period of time
- The results were analyzed in order to identify at what point in time a critical degree of degradation of .88 of the outer PVC insulation existed
- The time at which was defined as the predicted time for electrical cable arc failure for the specified temperature
- This was repeated for temperatures ranging from 100°C to 300°C

Figures 40 and 41 portray the model predictions of time to failure of the cable at various temperatures. Figure 40 shows the three experimental data points used to calibrate the model as

well as 13 of the 18 temperatures used in the model. Figure 41 is included to show the error (two standard deviations of the mean) associated with each testing data point. These times to failure were initially used to model an energized, unloaded cable with a prescribed environmental temperature. In the unloaded experiments, the environmental temperature and the internal cable temperature were said to be the same. In addition to the temperatures shown in Figure 40, lower temperatures were modeled as well and included in the development of the curve shown. Some of the lower temperatures modeled were 100°C, 125°C, and 150°C (Not shown for graphing/scale purposes) The predicted time to failure for these temperatures was approximately 20 years, 1 year, and 28 days, respectively. All model predictions are listed in the Appendix. In the previously conducted experiments with added insulation in a 100°C oven environment (up to 115°C within the cable), electrical arc failure was not exhibited during the 60 hours of testing. The predictions of this model at temperatures around 115°C corroborate the experimental result that electrical arc failure should not have been expected to occur within the 60 hour testing timeframe. In Figure 41 the error bars of the 210°C data point is seven minutes and is too small to see graphically.

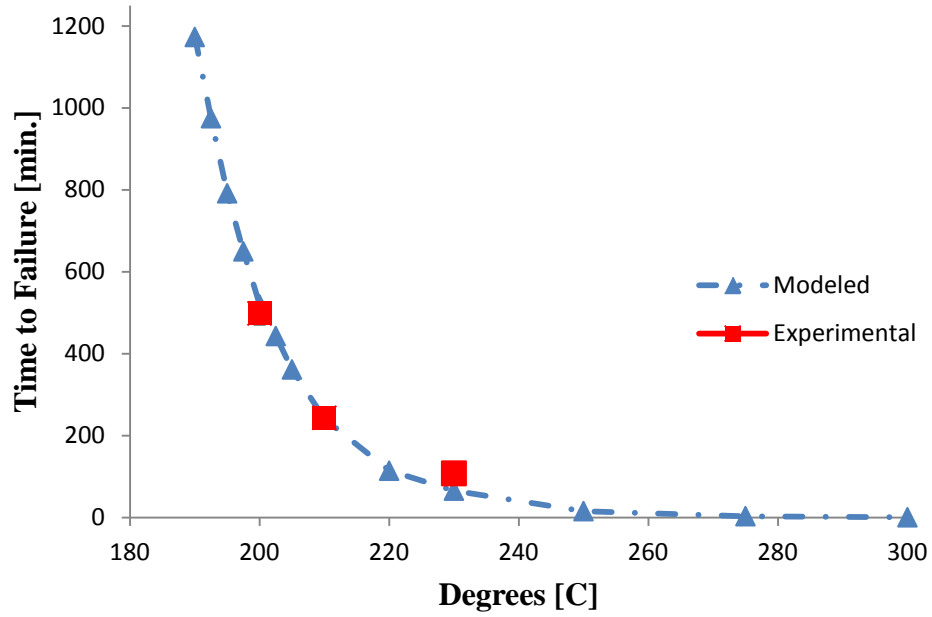


Figure 40: Model, Experimental Time to Failure Predictions (1)

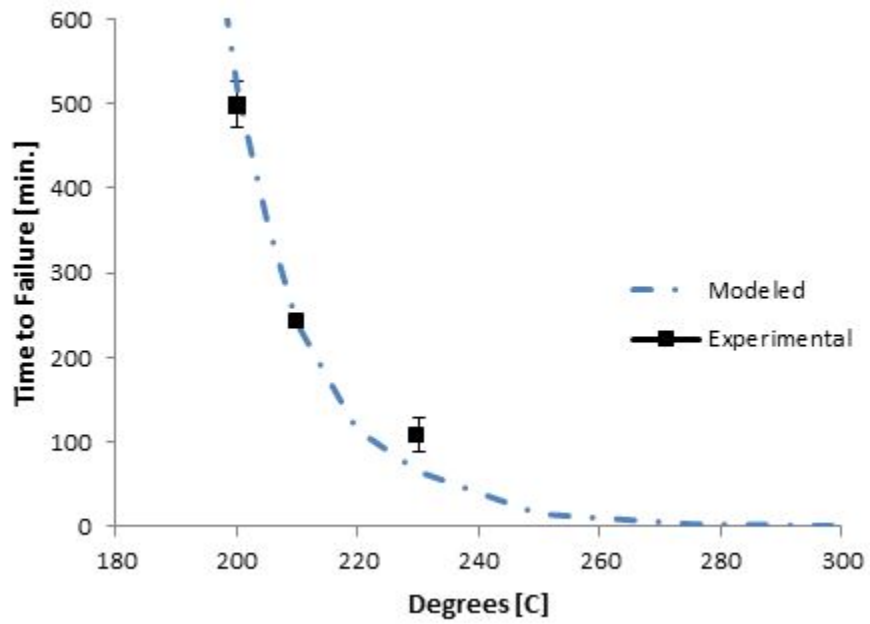


Figure 41: Model, Experimental Time to Failure Predictions (2)

As previously mentioned, an additional increase in internal cable temperature was seen when a load was introduced to the cable. Therefore, it was hypothesized that the increase in cable temperature caused the decrease in time to arc failure in the different 200°C load scenarios as shown in Table 4. Furthermore, the increased cable temperatures of the loaded scenarios were inputted into the model previously used to represent the unloaded scenarios (in which the environmental temperature and cable temperature were found to be relatively equal throughout the experiment). The temperatures used for input for the loaded scenarios were average steady-state cable temperatures calculated after the cable reached the prescribed oven atmospheric temperature and up until arc failure. The temperatures are those listed in Table 5. Figure 42 shows the previously developed model along with the time to arc failure predicted by the model for the load scenarios. The model slightly over-predicts the time to failure for the energized and loaded cable scenarios. One reason for this may be because the temperature measurements were taken just underneath the outer PVC insulation. It is assumed that closer to the actual current flow in the interior of the cable, there is a higher temperature. Therefore, if the temperatures from the middle of the cable were able to be obtained and used to compare with the modeled prediction, a closer agreement would exist. However, in an attempt to cause as little disruption to the cable geometry as possible, taking temperature measurements at the center of the cable was not feasible.

In the loaded cable experiments, an increase in temperature was seen in the last minutes before an electrical arc failure. For the 12 Amp tests, this was observed over a longer time frame than for the 18 Amps tests which produced noticeable increase in temperature in the last minutes before the arc failure occurred. If the cable temperature is re-averaged for the last three minutes before the arc failure, the average temperature slightly increases and is shown in Table 12. If

these temperature measurements are used to compare against the model, slightly better agreement exists. The model still slightly over predicts the time to failure for the loaded scenarios, but to a lesser degree. The loaded scenarios with re-averaged temperatures and the model are displayed in Figure 43. The error estimate used is based off the standard deviations for the non-loaded scenarios.

Table 12: Energied, Loaded Cable Temperature Corrections

	200°C – 12 Amps	200°C – 18 Amps
Avg. After Steady State	202	204
Avg. of Final 3 Minutes	203.4	206.7

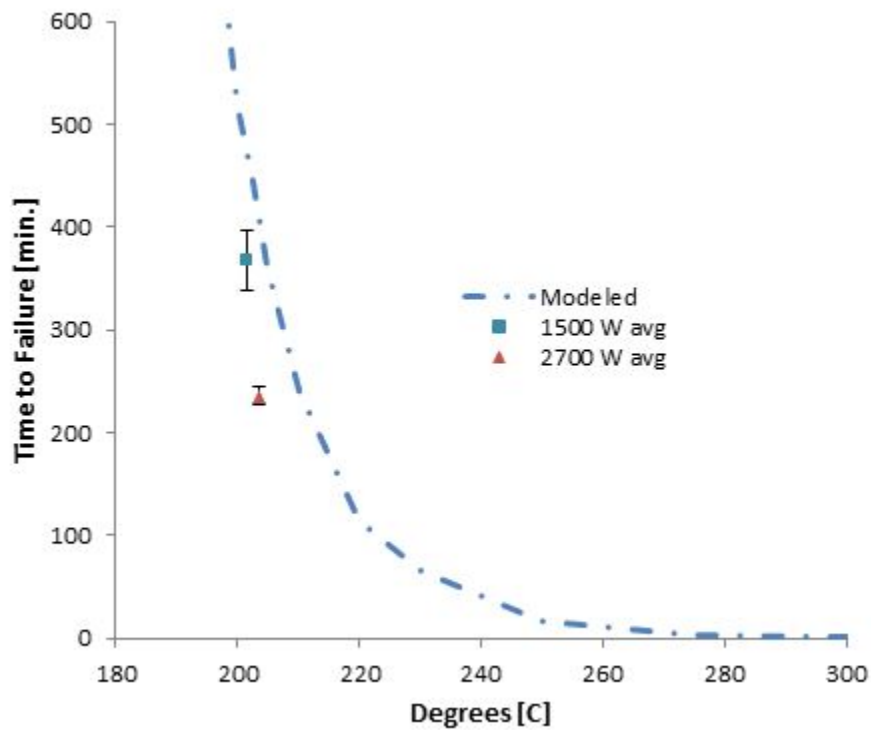


Figure 42: Model, Loaded Experimental Time to Failure Predictions

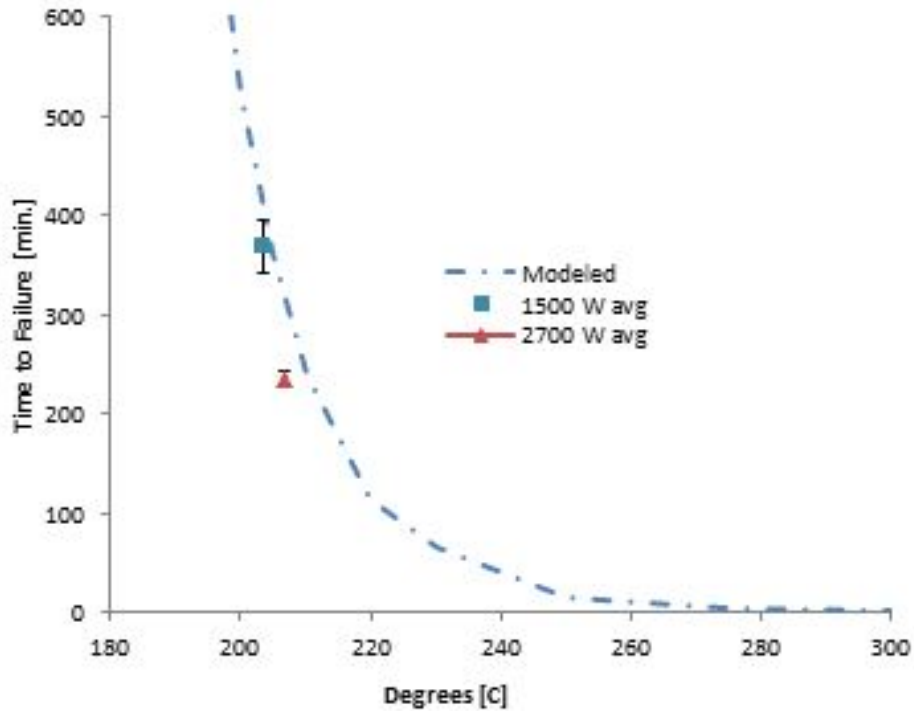


Figure 43: Correct Model, Loaded Experimental Time to Failure Predictions

5 CONCLUSIONS

The purpose of this study was to examine thermally induced electrical arcing failure in residential cables. To do this, several testing methodologies were developed to examine different aspects of electrical arcing behavior in residential cables under thermal conditions. The cable studied was Southwire Romex Simpull non-metallic sheathed 14/2 AWG with ground cable. The cable and its insulation components were subjected to a variety of temperatures with the time to arc failure as the main piece of data recorded. As compared to previous studies performed on the subject, a slower and more uniform heating approach was used and is believed to be a better representation of how cable insulations may experience thermal degradation over time and lead to electric arc failure [6,7,8,15]. This may allow for better extrapolation of data to a wider range of thermal hazards over a prolonged time period. A pyrolysis model utilizing a

thermally thin assumption was then developed to model PVC insulation degradation, and in turn predict time to electric arc failure of the cable.

The model developed was successful in predicting/verifying the time to arc failure of the cable used in the experiments. The model was able to predict electrical arc failure under thermal conditions for the cables used in these experiments based upon an experimentally determined critical degree of degradation of the PVC insulation in the cables. For the energized, unloaded cable experiments, the model was able to better predict the time to failure at lower temperatures (200°C and 210°C) in which the temperature ramps were a less significant part of the exposure. The experimental results differed from the model by less than 5% in these cases. For the 230°C energized, unloaded scenario, the experimental results differed from the model by about 35%. This is believed to be due to the fact that the heating process accounted for almost half of the thermal exposure time for these scenarios. Therefore, the model is more successful in predicting time to failure for a steady thermal exposure. The experimental time to arc failures for the 200°C 12 Amp for the 200°C 18 Amp loaded tests differed from the model by 8% and 25%, respectively.. Had the temperature of the interior of the cable been able to be measured, the agreement between the experimental and modeled time to failure for a given temperature would become stronger. Additionally, the model was used to extrapolate the data to temperatures not tested in experimentation.

The fact that the cables were exposed to steady temperatures for extended periods of time before exhibiting electrical arc failure demonstrates that the arc failure is affected by both temperature and the length of time of exposure. This finding is fundamentally different than that of previous studies on the subject that suggest that the arc failure occurs when the PVC insulation reaches a specified critical temperature. Previous studies do not take into account that

the time of thermal exposure affects when an electric arc failure will occur [6,7,8,9]. The results of this study support the notion that the temperature and the time of exposure are both critical factors leading up to electrical arc failure and must both be considered when predicting arc failure.

6 FUTURE WORKS

The conclusions of this research are powerful in beginning to gain a better understanding of thermally induced arcing failure of electrical cables. There are a few limitations of the findings of this study. One limitation is the application of the developed pyrolysis model to other types of cables. The experiments were performed on one specific type of cable and at this point, the results of this study can only be applied to the specific cable tested. Another limitation exists in that the cables tested were all new, previously unused rolls of cable. Therefore, the results should not be used to offer any conclusions about aged cables. The results may vary for cables that have encountered significant aging.

During and after completion of this study, several areas were identified as possible areas of future work. One area would be in testing additional types and brands of electrical cables. Currently, the results of this study should not be used to make any definitive statements about other types of electrical cables. Also, doing extended testing at temperatures lower than those selected for this study would be valuable.

In order to gain a better understanding of the recorded internal cable temperatures, additional thermocouples should be introduced into the testing set up. This will allow for a greater understanding of the temperature increases realized within the cable. Also, more resolved current measurements should be performed to attempt to understand the possible

existence of a “leak” current prior to an electrical arc failure. This may correlate with the increased temperatures recorded prior to arcing failure.

APPENDIX

ThermaKin Input File Examples

Components Example – 200°C Outer PVC

```
COMPONENT:      PVC
STATE:          S
DENSITY:        1150  0  0  0
HEAT CAPACITY:  601.4  3.63  0  0
CONDUCTIVITY:   0.25  0  0  0
TRANSPORT:      1e-5  0  0  0
EMISSIVITY & ABSORPTION:  0  1.5
```

```
COMPONENT:      PVC_ch
STATE:          S
DENSITY:        1180  0  0  0
HEAT CAPACITY:  -405.26  1.07  0  0
CONDUCTIVITY:   0.25  0  0  0
TRANSPORT:      1e-5  0  0  0
EMISSIVITY & ABSORPTION:  0  1.5
```

```
COMPONENT:      PVC_g
STATE:          G
DENSITY:        1180  0  0  0
HEAT CAPACITY:  1900  0  0  0
CONDUCTIVITY:   0.25  0  0  0
TRANSPORT:      1e-5  0  0  0
EMISSIVITY & ABSORPTION:  0  1.5
```

MIXTURES

```
S SWELLING:      0
L SWELLING:      0
G SWELLING LIMIT:  1e-30
PARALL CONDUCTIVITY:  0.5
PARALL TRANSPORT:  0.5
```

```
REACTION:        PVC + NOCOMP -> PVC_ch + PVC_g
STOICHIOMETRY:   1    0          0.48    0.52
ARRHENIUS:       7.98e10  145000
HEAT:            0  0  0  0
TEMP LIMIT:      L  300
```

Conditions Example – 200°C Outer PVC

OBJECT TYPE: 1D

OBJECT STRUCTURE

THICKNESS: 5e-5
TEMPERATURE: 313
MASS FRACTIONS:
PVC 1

OBJECT BOUNDARIES

TOP BOUNDARY

MASS TRANSPORT: YES
PVC_g LIN 0.05 0

OUTSIDE TEMP TIME PROG: 473 0
CONVECTION COEFF: 1e5

EXTERNAL RADIATION: NO

FLAME: NO

BOTTOM BOUNDARY

MASS TRANSPORT: NO

OUTSIDE TEMP TIME PROG: 473 0
CONVECTION COEFF: 1e5

EXTERNAL RADIATION: NO

FLAME: NO

INTEGRATION PARAMETERS

ELEMENT SIZE: 1e-5
TIME STEP: 0.01
DURATION: 31000

OUTPUT FREQUENCY:
ELEMENTS: 1
TIME STEPS: 1000

Components Example – 200°C Outer PVC

COMPONENT: PVCi
STATE: S
DENSITY: 1150 0 0 0
HEAT CAPACITY: 601.4 3.63 0 0
CONDUCTIVITY: 0.25 0 0 0
TRANSPORT: 1e-5 0 0 0
EMISSIVITY & ABSORPTION: 0 1.5

COMPONENT: PVCi_ch
STATE: S
DENSITY: 1180 0 0 0
HEAT CAPACITY: -405.26 1.07 0 0
CONDUCTIVITY: 0.25 0 0 0
TRANSPORT: 1e-5 0 0 0
EMISSIVITY & ABSORPTION: 0 1.5

COMPONENT: PVCi_g
STATE: G
DENSITY: 1180 0 0 0
HEAT CAPACITY: 1900 0 0 0
CONDUCTIVITY: 0.25 0 0 0
TRANSPORT: 1e-5 0 0 0
EMISSIVITY & ABSORPTION: 0 1.5

MIXTURES

S SWELLING: 0
L SWELLING: 0
G SWELLING LIMIT: 1e-30
PARALL CONDUCTIVITY: 0.5
PARALL TRANSPORT: 0.5

REACTION: PVCi + NOCOMP -> PVCi_ch + PVCi_g
STOICHIOMETRY: 1 0 0.393 0.607
ARRHENIUS: 2.62e11 152000
HEAT: 0 0 0 0
TEMP LIMIT: L 300

Conditions Example – 200°C Outer PVC

OBJECT TYPE: 1D

OBJECT STRUCTURE

THICKNESS: 5e-5
TEMPERATURE: 313
MASS FRACTIONS:
PVCi 1

OBJECT BOUNDARIES

TOP BOUNDARY

MASS TRANSPORT: YES
PVCi_g LIN 0.05 0

OUTSIDE TEMP TIME PROG: 473 0
CONVECTION COEFF: 1e5

EXTERNAL RADIATION: NO

FLAME: NO

BOTTOM BOUNDARY

MASS TRANSPORT: NO

OUTSIDE TEMP TIME PROG: 473 0
CONVECTION COEFF: 1e5

EXTERNAL RADIATION: NO

FLAME: NO

INTEGRATION PARAMETERS

ELEMENT SIZE: 1e-5
TIME STEP: 0.01
DURATION: 31000

OUTPUT FREQUENCY:
ELEMENTS: 1
TIME STEPS: 1000

Components Example – 200°C Nylon

COMPONENT: NYLON
STATE: S
DENSITY: 1150 0 0 0
HEAT CAPACITY: 601.4 3.63 0 0
CONDUCTIVITY: 0.25 0 0 0
TRANSPORT: 1e-5 0 0 0
EMISSIVITY & ABSORPTION: 0 1.5

COMPONENT: NYLON_ch
STATE: S
DENSITY: 1180 0 0 0
HEAT CAPACITY: -405.26 1.07 0 0
CONDUCTIVITY: 0.25 0 0 0
TRANSPORT: 1e-5 0 0 0
EMISSIVITY & ABSORPTION: 0 1.5

COMPONENT: NYLON_g
STATE: G
DENSITY: 1180 0 0 0
HEAT CAPACITY: 1900 0 0 0
CONDUCTIVITY: 0.25 0 0 0
TRANSPORT: 1e-5 0 0 0
EMISSIVITY & ABSORPTION: 0 1.5

MIXTURES

S SWELLING: 0
L SWELLING: 0
G SWELLING LIMIT: 1e-30
PARALL CONDUCTIVITY: 0.5
PARALL TRANSPORT: 0.5

REACTION: NYLON + NOCOMP -> NYLON_ch + NYLON_g
STOICHIOMETRY: 1 0 0.052 0.948
ARRHENIUS: 2.30e18 281053
HEAT: 0 0 0 0
TEMP LIMIT: L 300

Conditions Example – 200°C Nylon

OBJECT TYPE: 1D

OBJECT STRUCTURE

THICKNESS: 5e-5
TEMPERATURE: 313
MASS FRACTIONS:
NYLON 1

OBJECT BOUNDARIES

TOP BOUNDARY

MASS TRANSPORT: YES
NYLON_g LIN 0.05 0

OUTSIDE TEMP TIME PROG: 473 0
CONVECTION COEFF: 1e5

EXTERNAL RADIATION: NO

FLAME: NO

BOTTOM BOUNDARY

MASS TRANSPORT: NO

OUTSIDE TEMP TIME PROG: 473 0
CONVECTION COEFF: 1e5

EXTERNAL RADIATION: NO

FLAME: NO

INTEGRATION PARAMETERS

ELEMENT SIZE: 1e-5
TIME STEP: 0.01
DURATION: 29000

OUTPUT FREQUENCY:
ELEMENTS: 1
TIME STEPS: 1000

Components Example – 200°C Paper

COMPONENT: Paper
STATE: S
DENSITY: 500 0 0 0
HEAT CAPACITY: 601.4 3.63 0 0
CONDUCTIVITY: 0.25 0 0 0
TRANSPORT: 1e-5 0 0 0
EMISSIVITY & ABSORPTION: 0 1.5

COMPONENT: Paper_ch
STATE: S
DENSITY: 1180 0 0 0
HEAT CAPACITY: -405.26 1.07 0 0
CONDUCTIVITY: 0.25 0 0 0
TRANSPORT: 1e-5 0 0 0
EMISSIVITY & ABSORPTION: 0 1.5

COMPONENT: Paper_g
STATE: G
DENSITY: 1180 0 0 0
HEAT CAPACITY: 1900 0 0 0
CONDUCTIVITY: 0.25 0 0 0
TRANSPORT: 1e-5 0 0 0
EMISSIVITY & ABSORPTION: 0 1.5

MIXTURES

S SWELLING: 0
L SWELLING: 0
G SWELLING LIMIT: 1e-30
PARALL CONDUCTIVITY: 0.5
PARALL TRANSPORT: 0.5

REACTION: Paper + NOCOMP -> Paper_ch + Paper_g
STOICHIOMETRY: 1 0 0.219 0.781
ARRHENIUS: 2.40e15 212000
HEAT: 0 0 0 0
TEMP LIMIT: L 300

Conditions Example – 200°C Paper

OBJECT TYPE: 1D

OBJECT STRUCTURE

THICKNESS: 5e-5
TEMPERATURE: 313
MASS FRACTIONS:
Paper 1

OBJECT BOUNDARIES

TOP BOUNDARY

MASS TRANSPORT: YES
Paper_g LIN 0.05 0

OUTSIDE TEMP TIME PROG: 473 0
CONVECTION COEFF: 1e5

EXTERNAL RADIATION: NO

FLAME: NO

BOTTOM BOUNDARY

MASS TRANSPORT: NO

OUTSIDE TEMP TIME PROG: 473 0
CONVECTION COEFF: 1e5

EXTERNAL RADIATION: NO

FLAME: NO

INTEGRATION PARAMETERS

ELEMENT SIZE: 1e-5
TIME STEP: 0.01
DURATION: 29000

OUTPUT FREQUENCY:
ELEMENTS: 1
TIME STEPS: 1000

ThermaKin Model Predictions

Testing Temperature (C)	Predicted Time to Arc Failure (minutes)
100	10,550,000 (\approx 20 years)
125	556666.7 (\approx 1 year)
150	41666.7 (\approx 28 days)
175	4183
185	1614.8
190	1173.3
192.5	975
195	791.7
197.5	650
200	520.6 (actual = 498.5)
202.5	443.3
205	361.7
210	240.4 (actual = 243.7)
220	114.5
230	65.9 (actual = 108)
250	15.8
275	3.5
300	.867

Table 13: Model Time to Failure Predictions

Additional Pictures



Figure 43: Bubbled, Cracked Inner Insulation (Post Exposure)



Figure 44: Bubbled, Cracked Outer Insulation (Post Exposure)



Figure 45: Interior Cable Structure

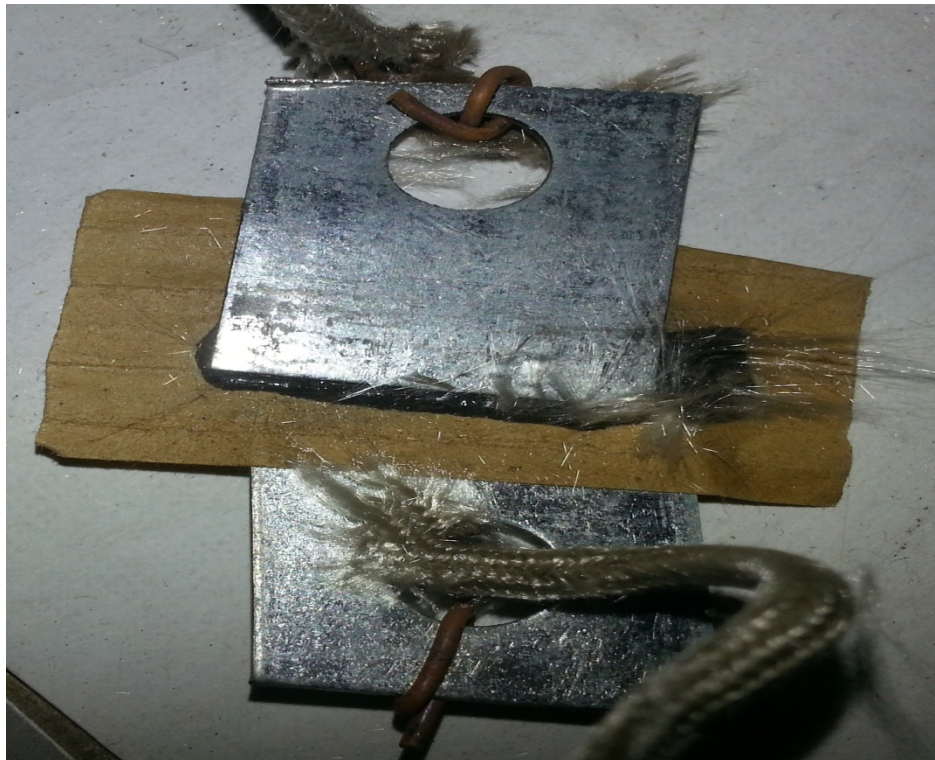


Figure 46: Component Testing Setup



Figure 47: Post Arc Failure (Destroyed hot and ground wires)

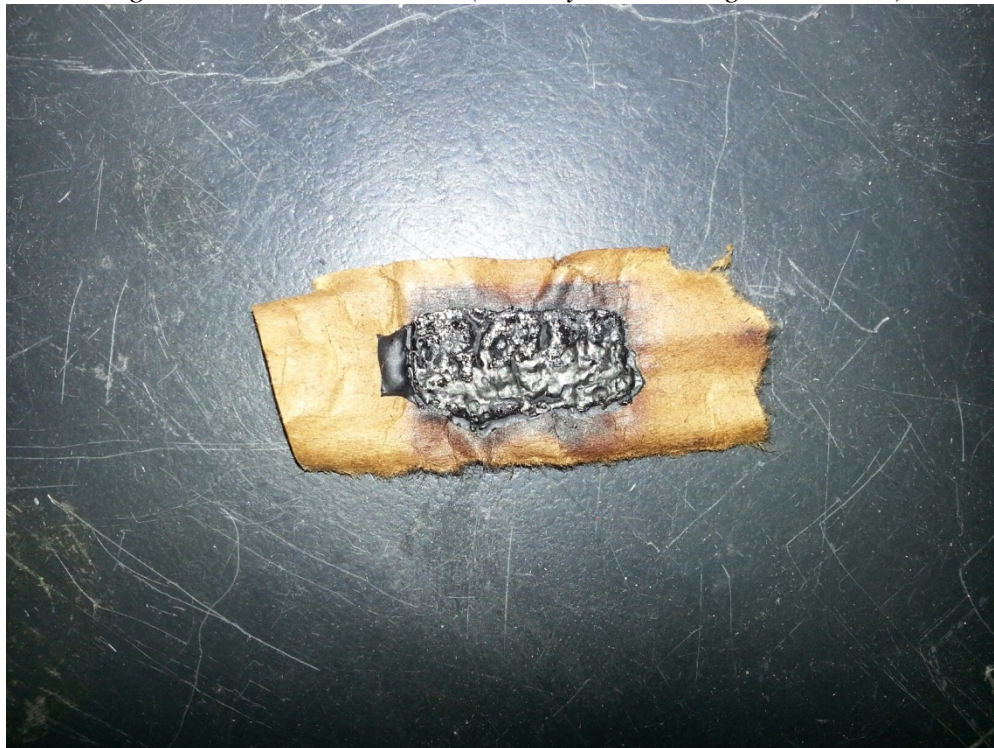


Figure 48: PVC-Paper Combination Testing (Post Exposure)



Figure 49: Copper Beads Ejected From Cable During Arc Failure

230°C Full Cable Resistance Drop Testing Results

Test Number	Time to Arc Failure (min.)
1	70.0
2	68.3
3	83.3
4	71.4
5	83.8
6	66.5
7	60.7

200°C Energized, Non-loaded Full Cable Time to Arc Failure Results

Test Number	Time to Arc Failure (min.)
1	486.3
2	505.5
3	510.7
4	494.8
5	522.1
6	524.1
7	500.7

210°C Energized, Non-loaded Full Cable Time to Arc Failure Results

Test Number	Time to Arc Failure (min.)
1	240.2
2	240.3
3	231.0
4	245.1
5	260.9
6	237.3
7	244.15

230°C Energized, Non-loaded Full Cable Time to Arc Failure Results

Test Number	Time to Arc Failure (min.)
1	97.2
2	98.2
3	97.1
4	166.5
5	97.5
6	103.9
7	97.2

200°C Energized 18 Amps Loaded Full Cable Time to Arc Failure Results

Test Number	Time to Arc Failure (min.)
1	251.0
2	237.9
3	220.3
4	225.9
5	235.1
6	227.3
7	252.8

230°C Outer PVC Time to Resistance Drop, Time to Arcing Results

Outer PVC Test Number	Time to Res. Drop (min.)
1	46.3
2	54.3
3	46.5
4	35.7
5	44.3
6	51.4
7	49.2

230°C Inner PVC Time to Resistance Drop, Time to Arcing Results

Inner PVC Test Number	Time to Res. Drop (min.)
1	49.4
2	38.1
3	44.4
4	39.9
5	40.8
6	37.1
7	42.2

230°C Nylon Time to Resistance Drop, Time to Arcing Results

Nylon Test Number	Time to Res. Drop (min.)
1	60.1
2	50.7
3	47.7
4	52.5
5	39.5
6	44.0
7	47.6

230°C PVC-Paper Combination Time to Resistance Drop Results

PVC/Paper Test Number	Time to Res. Drop (min.)
1	73.6
2	79.7
3	-
4	-
5	-
6	92.7
7	-
8	84.8
9	-
10	94.6
11	88.1
12	-
13	-
14	71.4
15	-
16	-
17	-
18	-
19	-
20	-
21	76.4
22	-
23	72.5
24	-
25	-
26	-
27	90.9
28	-
29	99.6
30	-
31	-
32	-
33	-
34	81.3
35	-
36	111.6
37	-
38	-
39	-

200°C Full Cable - Tight Arrangement Time to Arc Failure Results

Test Number	Time to Failure (min.)
1	519.9
2	530.2
3	509.5
4	524.9
5	537.9

230°C Full Cable- Removed Ground Paper Sheathing Time to Arc Failure

Test Number	Time to Arc Failure (min.)
1	82.4
2	59.2
3	57.7
4	92.2
5	93.9
6	93.8
7	85.9

Loaded, Insulated Time to Arc Failure

	Time to Arc Failure
100°C, 12 Amps	<60 hours

REFERENCES

- [1] Miller, David. Chowdhury, Risana. “2006-2008 Residential Fire Loss Estimates”. *U.S. National Estimates of Fires, Deaths, Injuries, and Property Losses from Unintentional Fires*. July 2011.
- [2] “Residential Building Electrical Fires”. United States Fire Administration. *Tropical Fire Report Series*. Vol. 8 Issue 2. March 2008.
- [3] V. Babrauskas, "Electrical Fires," in *SFPE Handbook of Fire Protection Engineering*, Quincy, National Fire Protection Association, 2008, pp. 479 - 498.
- [4] Novak, Cameron. “An Analysis of Heat Flux-Induced Arc Formation In Residential Electrical Cables”. University of Maryland. 2011.
- [5] Barbauskas, V. “Fires due to Electrical Arcing: Can ‘Cause Beads Be Distinguished from ‘Victim’ Beads by Physical or Chemical Testing?”. *Fire and Materials* 2003. Pp. 189-201. 2003.
- [6] “Cable Response to Live Fire (CAROLFIRE) Volume 1: Test Descriptions and Analysis of Circuit Response Data”. United States Nuclear Regulatory Commission. Vol. 1. April 2008.
- [7] “Cable Response to Live Fire (CAROLFIRE) Volume 2: Cable Fire Response Data for Fire Model Improvement”. United States Nuclear Regulatory Commission. Vol. 2. April 2008.
- [8] “Cable Response to Live Fire (CAROLFIRE) Volume 3: Thermally-Induced Electrical Failure (THIEF) Model”. National Institute of Standards and Technology. United States Nuclear Regulatory Commission . Vol. 3. April 2007.
- [9] Matala, Anna. Hostikka, Simo. “Probabilistic Simulation of Cable Fires in a Cable Tunnel”. 20th International Conference on Structural Mechanics in Reactor Technology (SMiRT 20). 11th international Post Conference Seminar on ‘Fire Safety in Nuclear Power Plants and Installations’. Espoo, Finland.
- [10] Shea, John J. “Identifying causes for certain types of electrically initiated fires in residential circuits”. *Fire and Materials*. 19 July 2010.
- [11] “Copper Building Wire”. Southwire. Romex SIMpull Type NM-B. pp.10.
- [12] National Electric Code. National Fire Protection Association (NFPA) 70 2011 Edition.
- [13] Rudd, Armin. Lsitburke, Joseph. “Measurement of Attic Temperatures and Cooling Energy Use in Vented and Sealed Attics in Las Vegas, Nevada. Nov 1996.
- [14] Li, Jing. Stoliarov, Stanislav I. “ Measurement of kinetics and thermodynamics of the thermal degradation of non-charring polymers”. *Combustion and Flame*. March 2013.
- [15] Novak C.J.; Stoliarov S. I.; Keller M. R.; Quintiere J. G.: “Analysis of Heat Flux Induced Arc Formation in a Residential Electrical Cable. *Fire Safety Journal*; Vol. 55. pp. 61-68 (2013)

- [16] S. I. Stoliarov and R. E. Lyon, "Technical Note: Thermo-Kinetic Model of Burning," U.S. Department of Transportation - Federal Aviation Administration, Springfield, 2008.
- [17] S. Stoliarov, S. Crowley, R. Walters and R. Lyon, "Prediction of the Burning Rates of Charring Polymers," *Combustion and Flame*, vol. 157, no. 11, pp. 2024-2034, 2010.
- [18] Benes, M. Milanov, N. Matuschek, G., Kettrup, A. Placek, V. Balek, V. "Thermal Degradation of PVC Cable Insulation Studied by Simultaneous TG-FTIR and TG-EGA Methods". *Journal of Thermal Analysis and Calorimetry*. Vol. 78. pp. 621-630. 2004.
- [19] Wang, Nam Sun. "Cellulose Degradation: Experiment 4". Department of Chemical and Biological Engineering. University of Maryland.